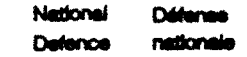

A FAST FOURIER TRANSFORM APPROACH TO INTERFERENCE SUPPRESSION IN DIRECT SEQUENCE SPREAD SPECTRUM SIGNALS

by

Brian Kozminchuk

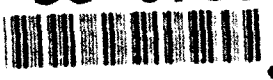

DEFENCE RESEARCH ESTABLISHMENT OTTAWA
TECHNICAL NOTE 93-2

Canada

December 1992
Ottawa

National Defence / Défense nationale

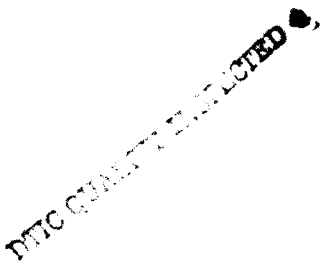

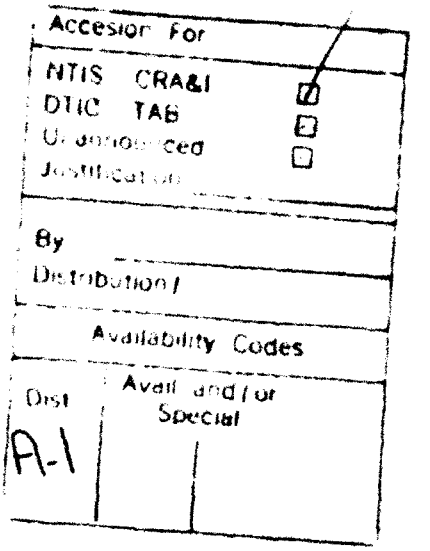

A FAST FOURIER TRANSFORM APPROACH TO INTERFERENCE SUPPRESSION IN DIRECT SEQUENCE SPREAD SPECTRUM SIGNALS

by

Brian Kozminchuk
Communications Electronic Warfare Section
Electronic Warfare Division

DEFENCE RESEARCH ESTABLISHMENT OTTAWA
TECHNICAL NOTE 93-2

PCN
041LK11

December 1992
Ottawa

ABSTRACT

An FFT algorithm is examined with respect to its utility as an interference suppressor in direct sequence spread spectrum communications signals. An FFT approach is especially attractive because of its computational economy. It is this approach which has been implemented on the TMS320C30 hardware forming part of the Advanced Communications Electronic Support Measures System (ACES) and will be implemented on other high-speed hardware forming part of that system. The basic problem to be solved is described, followed by a description of the algorithm. The algorithm consists of power spectrum estimation using an FFT-based routine, interpolation of the power spectrum at a set of equally-spaced points different from those calculated by the FFT, and design of an FIR linear phase filter which filters the data, i.e., suppresses the interference. This technique is feasible so long as the bandwidth of the interference during the observation time over which the FFT is calculated is much less than the bandwidth of the spread spectrum signal. An important result from this brief study is that the interpolation algorithm used can have an effect on the performance and reliability of the suppression filter ultimately designed and that for small order filters, the discrete Fourier transform approach may be better.

RÉSUMÉ

On examine un algorithme de transformée de Fourier rapide (FFT) pour déterminer son utilité pour supprimer de l'interférence sur des signaux de communications à spectre étalé par séquence directe. Cette approche par FFT apparaît particulièrement intéressante en raison de la faible quantité de calculs requis. Il s'agit en fait de l'approche sélectionnée pour le matériel utilisant le TMS320C30 incorporé au Système Avancé de Mesures de Soutien Electronique (SAMSE), de même que pour d'autres circuits à haute vitesse prévus pour ce même système. On décrit d'abord le problème fondamental à résoudre, puis l'algorithme choisi. Cet algorithme se fonde sur une estimation du spectre de puissance et procède par transformée de Fourier rapide à une interpolation du spectre de puissance sur une série de points équidistants, mais différents de ceux calculés par la transformée. L'algorithme génère un filtre FIR à phase linéaire, lequel permet la filtration des données et, par le fait même, la suppression de l'interférence. Cette technique demeure possible aussi longtemps que la largeur de bande de l'interférence, prévalant pendant la durée de l'observation correspondant au calcul de la FFT, est passablement plus petite que la largeur de bande du signal à spectre étalé. Quelques points importants se dégagent de cette courte étude: l'algorithme d'interpolation utilisé peut avoir un effet sur la performance

et la fiabilité du filtre tel qu'ultimement conçu et, pour des filtres d'ordre peu élevé, l'approche par transformée de Fourier discrète peut s'avérer la meilleure.

EXECUTIVE SUMMARY

This technical note presents an FFT-based technique for filtering narrowband interference from spread spectrum communications signals. These signals are used extensively in military communication systems. The technique described herein applies equally to both Electronic Support Measures (ESM) systems and direct sequence spread spectrum communication sytems. In the former application, the ESM system may be attempting to intercept the spread spectrum signal, but the narrowband interference may be hampering this effort. In the latter application, the spread spectrum communication system may require additional assistance to suppress the interference. Since the open literature has been devoted to this latter case, the material presented here focuses on this application.

One of the attributes of direct sequence spread spectrum communication systems is their ability to combat interference or intentional jamming by virtue of the system's processing gain inherent in the spreading and despreading process. The interference can be attenuated by a factor up to this processing gain. In some cases the gain is insufficient to effectively suppress the interferer, leading to a significant degradation in system performance as manifested by a sudden increase in bit error rate. If the ratio of interference bandwidth to spread spectrum bandwidth is small, the interference can be filtered out to enhance system performance. However, this is at the expense of introducing some distortion onto the signal. This process of filtering is sometimes referred to as interference excision.

The FFT approach described herein is especially attractive because of its computational economy. It is this approach which has been implemented on the TMS320C30 hardware forming part of the Advanced Communications Electronic Support Measures System (ACES) and will be implemented on other high-speed hardware forming part of that system. The algorithm consists of power spectrum estimation using an FFT-based routine, interpolation of the power spectrum at a set of equally-spaced points different from those calculated by the FFT, and design of an FIR linear phase filter which filters the data, i.e., suppresses the interference. This technique is feasible so long as the bandwidth of the interference during the observation time over which the FFT is calculated is much less than the bandwidth of the spread spectrum signal.

There are two important results from this brief study. The first is that the interpolation algorithm and, to some extent, the window weighting used can have an effect on the performance and reliability of the suppression filter ultimately designed. The second is that for small filter orders, the discrete Fourier transform approach may be better, since for this latter case the interpolation algorithm would not be necessary.

TABLE OF CONTENTS

LIST OF FIGURES

1.0 INTRODUCTION

The focus of this technical note is to explore an FFT-based technique applied to interference suppression in direct sequence spread spectrum communications signals. This technique first appeared in a paper written by Ketchum and Proakis [1] in which several adaptive filtering algorithms were examined to address this problem.

The algorithms that were considered fit into two categories: non-parametric, i.e., DFT- or FFT-based, since no *a priori* knowledge of the interference is assumed, and parametric, i.e., algorithms based on linear prediction, in which the interference is assumed to be modelled as an autoregressive process.

The FFT approach to interference suppression is of practical importance because of the processing speed afforded by the FFT algorithm compared to the discrete Fourier transform (DFT), and the existence of high-speed DSP hardware currently available to calculate the FFT. In fact, it is this latter approach which has been implemented on the Advanced Communications Electronic Support Measures System (ACES) [2] using the TMS320C30[1] hardware therein. The experimental performance results from this latter system shall be presented in a future report. Furthermore, this technique will be implemented on the high-speed iWarp [2] processors which are also part of the ACES system.

The purpose of this technical note is to expand on the FFT-based approach and to spotlight possible problem areas, since the above mentioned paper did not elaborate much on this approach, nor did it present many performance results and potential pitfalls; it emphasized the parametric algorithms (Levinson-Durbin, Burg, and unconstrained block least squares). This technical note will be concerned with the following:

- the essence of the problem to be solved
- the communications model used in the simulations
- the algorithm which calculates the filter coefficients of the suppression filter
- simulation results, and
- concluding remarks.

[1]This is a Texas Instruments digital signal processing chip.
[2]This is an Intel product.

2.0 DESCRIPTION OF THE PROBLEM

One of the attributes of direct sequence or pseudo noise (PN) spread spectrum communications systems is their ability to combat interference or intentional jamming by virtue of the system's processing gain, which is the ratio of the signal's spread bandwidth to the underlying information bandwidth. The interference can be attenuated by a factor up to this processing gain, which may be in the range of up to 40 dB. In some cases, when the processing gain is insufficient to effectively suppress the interferer, communications will degrade significantly as manifested by a sudden increase in bit error rate. If the ratio of interference-bandwidth-to-spread-spectrum-bandwidth is small, the interference can be filtered out to enhance system performance. However, this is at the expense of introducing some distortion onto the signal. This filtering operation is based on the fact that, since the spectrum of the PN signal is relatively flat across the signal frequency band, a strong narrow-band interference is easil· recognized and estimated.

There are a host of digital techniques which can effect the estimation of the interference and its suppression. These digital techniques require that the received (spread) signal, noise and interference first be digitized. The resulting sequence is then applied to a digital filter which carries out the process of interference suppression. Its filter coefficients are obtained from an algorithm which, as described in the introduction, can be of the non-parametric or parametric type.

3.0 COMMUNICATIONS MODEL

The baseband (BPSK) communications model used in [1] is illustrated in Fig. 1. The basic elements of it will now be described.

At the transmitter, an information sequence, $D(t-kT_b)$, consisting of rectangular pulses of duration T_b and amplitude ± 1, is spread by a pseudo-random noise sequence, $PN(t - nT_c)$, consisting of rectangular chips of duration T_c ($T_c << T_b$ normally) and also of amplitude ± 1. The result is the baseband spread signal $s(t)$ which is applied to the channel.[3] The ratio of the chip rate $R_c = 1/T_c$ to the bit rate $R_b = 1/T_b$ is defined as the processing gain. Another definition of processing gain is the number of chips per bit, termed here as the variable L. For the simulations in this technical note, the chip

[3]The PN sequence is a deterministic signal and, therefore, has a spectrum consisting of discrete components. The envelope of the spectrum is described by a *sinc* function, with main-lobe of width $2R_c$; the discrete spectral lines are separated by $\Delta f = 1/(JT_c)$, where J refers to the number of chips in the period of the PN sequence. To obtain true spreading, the bandwidth of the information sequence must be greater than Δf.

duration will be $T_c = 1$ sec., implying that the energy/chip, E_c, will be equal to unity and the energy/bit, E_b will be equal to the processing gain L.

Examples of sections of the information sequence $D(t)$, the spreading sequence $PN(t)$, and the spread signal $s(t)$, and their respective power spectral densities are illustrated in Figs. 2 to 4. The parameters used to generate these figures are listed in Table 1

Table 1: Processing Parameters.

Parameter	Value
Bit rate, R_b	1/32 Hz
Chip rate, R_c	1 Hz
Sampling rate, f_s	8 Hz
Number of samples	16,384
FFT window	Rectangular
FFT sub-block size	512 points with 0 point overlapping

The power spectral density (PSD) was calculated using an FFT routine based on the Welch method [3].

Figure 2 illustrates a sequence of 64 bits and its PSD. Although difficult to determine from the figure, the bandwidth is approximately 2/32 Hz. Figure 3 illustrates a 256 second portion (2048 samples) of the spreading signal PN(t) and its PSD calculated from 16,384 samples. From the PSD, one can see that the main lobe is equal to twice the chip rate, i.e., $2R_c = 2$ Hz, with the nulls occurring at multiples of the chip rate[4]. Finally, Fig. 4 illustrates a section of the spread signal $s(t)$ of duration 256 seconds (8 bits) and

[4]A random number generator was used which has an extremely long period. This will result in a PN sequence which can be regarded as almost random, so that discrete spectral lines for the sequence do not appear.

its PSD. Close examination of the spectra in Figs. 3 and 4 shows slight differences as expected.

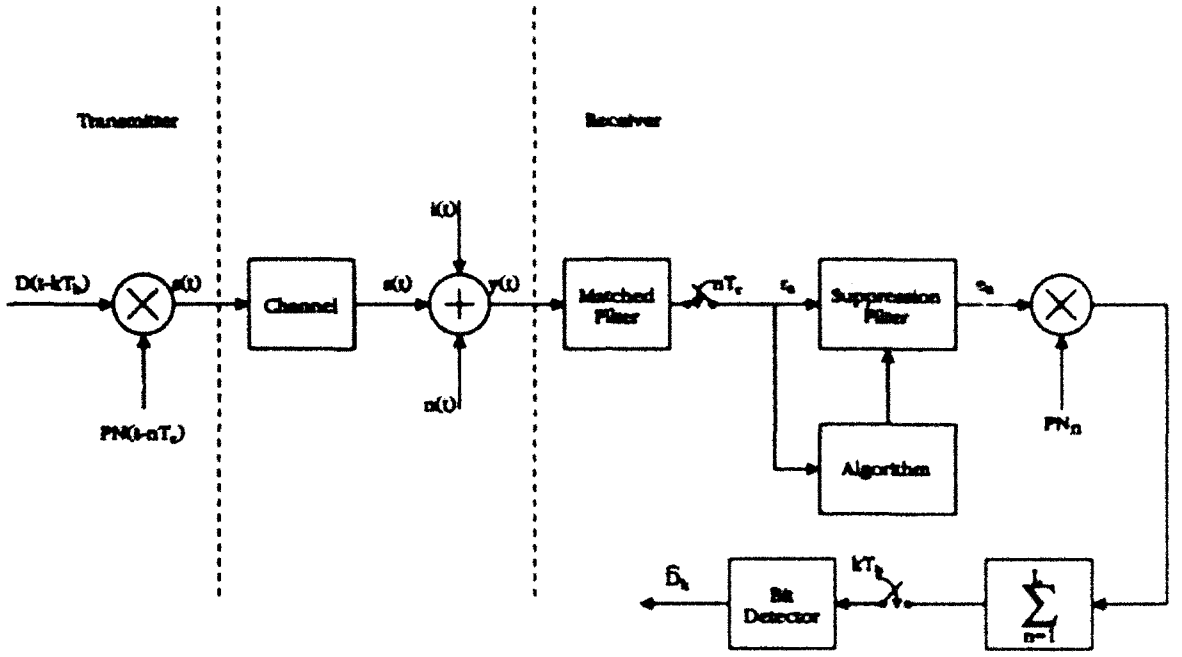

Figure 1: Baseband PN spread spectrum communications model.

In the communications model of Fig. 1, the signal $s(t)$ is transmitted over a channel. The channel considered in [1] was ideal, introducing no signal distortion. To the signal is added wide-band Gaussian noise with a two-sided PSD equal to $N_0/2$, and narrowband interference $i(t)$. Examples of the power spectra are illustrated in Figs. 5 and 6.

Figure 5 shows a section of signal plus noise for the condition $E_c/N_0 = -3.05$ dB. [5] Under these signal and noise conditions, the signal is only slightly visible. Figure 6 illustrates a portion of the same signal, but with interference added. The interference was a single tone located at a frequency of $f_i = 2/16$ Hz. The interference-power-to-spread signal-power (I/S) ratio for this example was 20 dB. Taking the spread signal power to be 1 unit, then with this ratio, the power P_i in the sinusoidal interference was 100 units.

Referring to the receiver section of Fig. 1, the composite signal, $y(t)$, consisting of signal, noise and interference, is applied to a matched filter (matched to a chip). For the

[5] This was obtained for an $E_b/N_0 = 12$ dB, so that, with the processing gain L equal to 32 chips/bit and $E_b = LE_c$, the desired result is obtained.

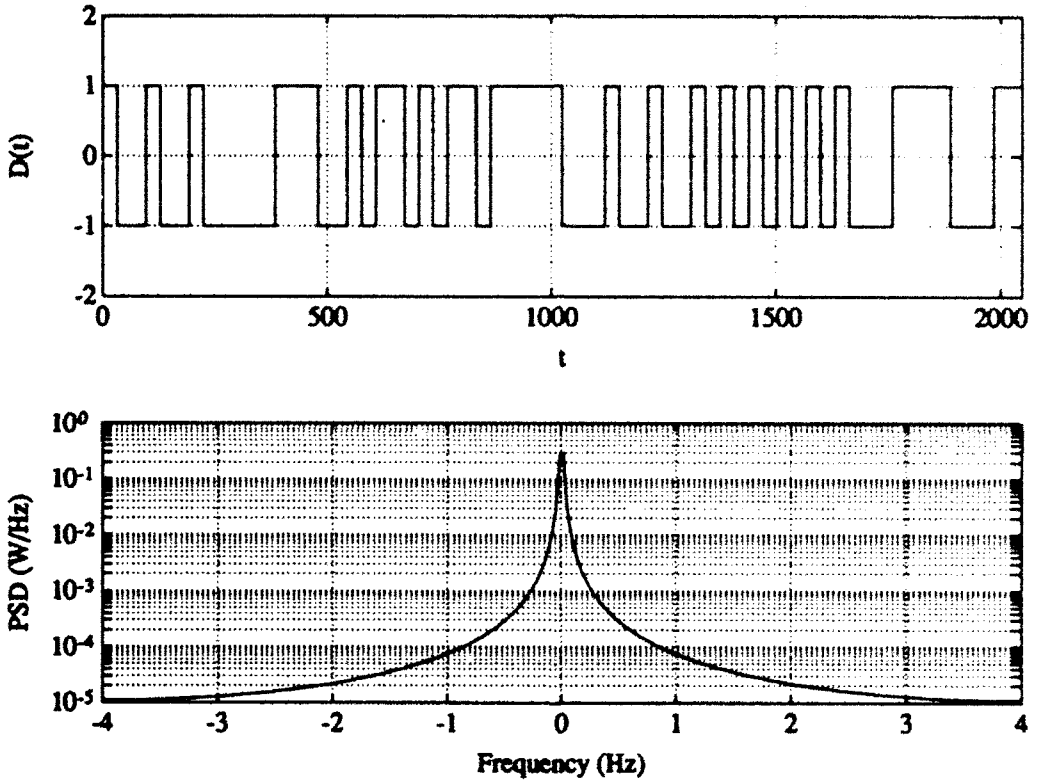

Figure 2: An example of a string of data bits and its power spectrum.

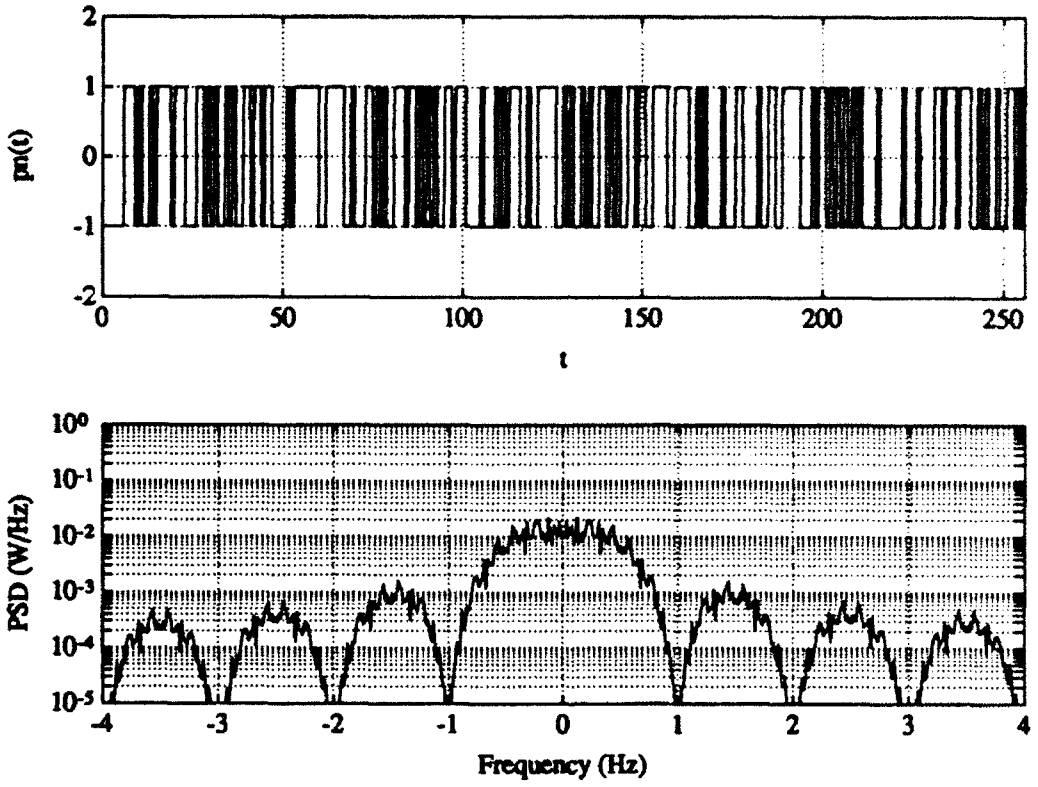

Figure 3: An example of a section of the pseudo-random sequence and its power spectrum.

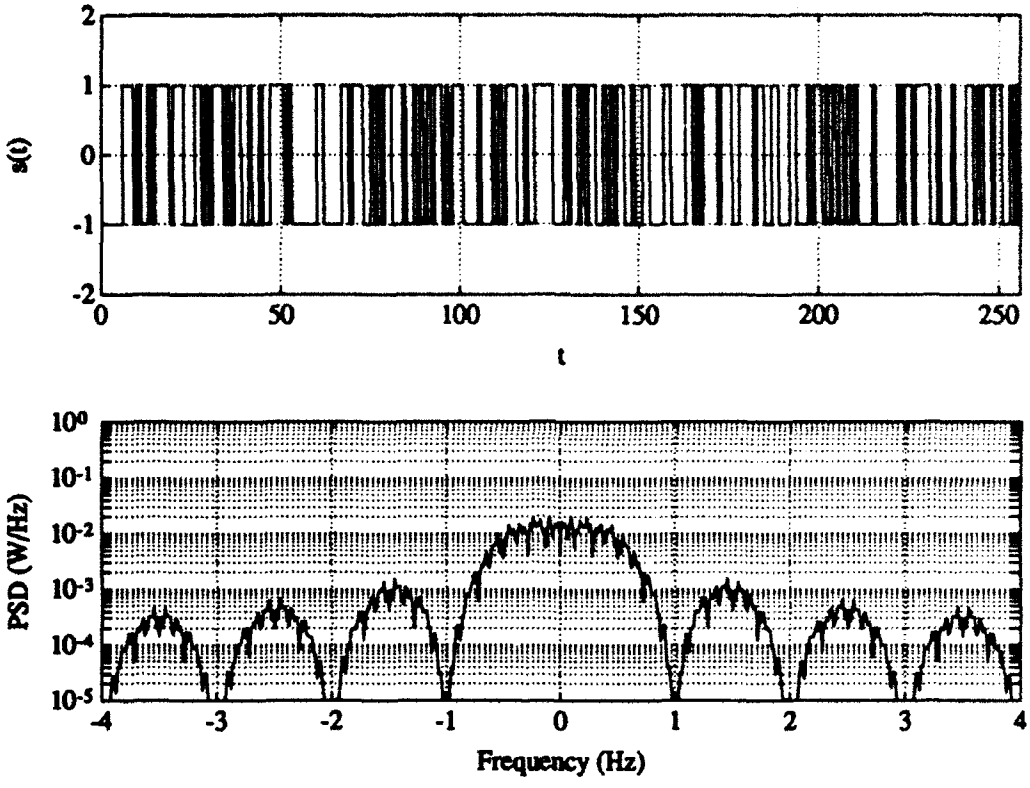

Figure 4: An example of the spread signal and its power spectrum, $E_c = 1$ unit.

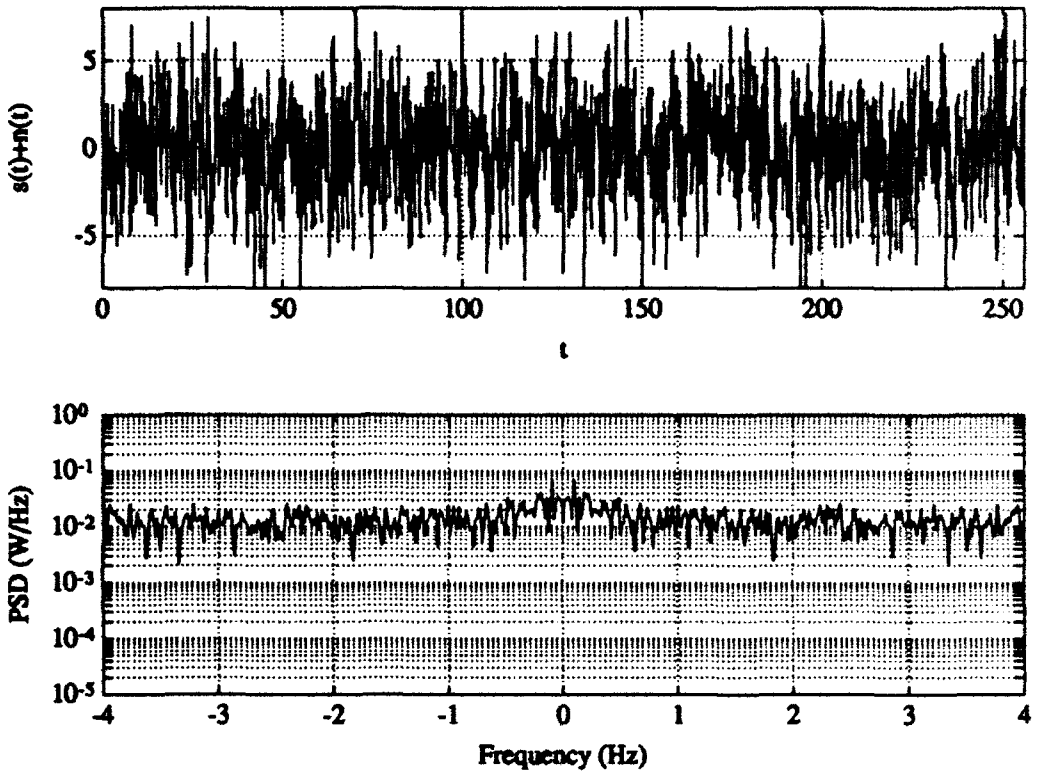

Figure 5: An example of the spread signal plus noise, and its power spectrum, $E_c/N_0 = -3.05$ dB.

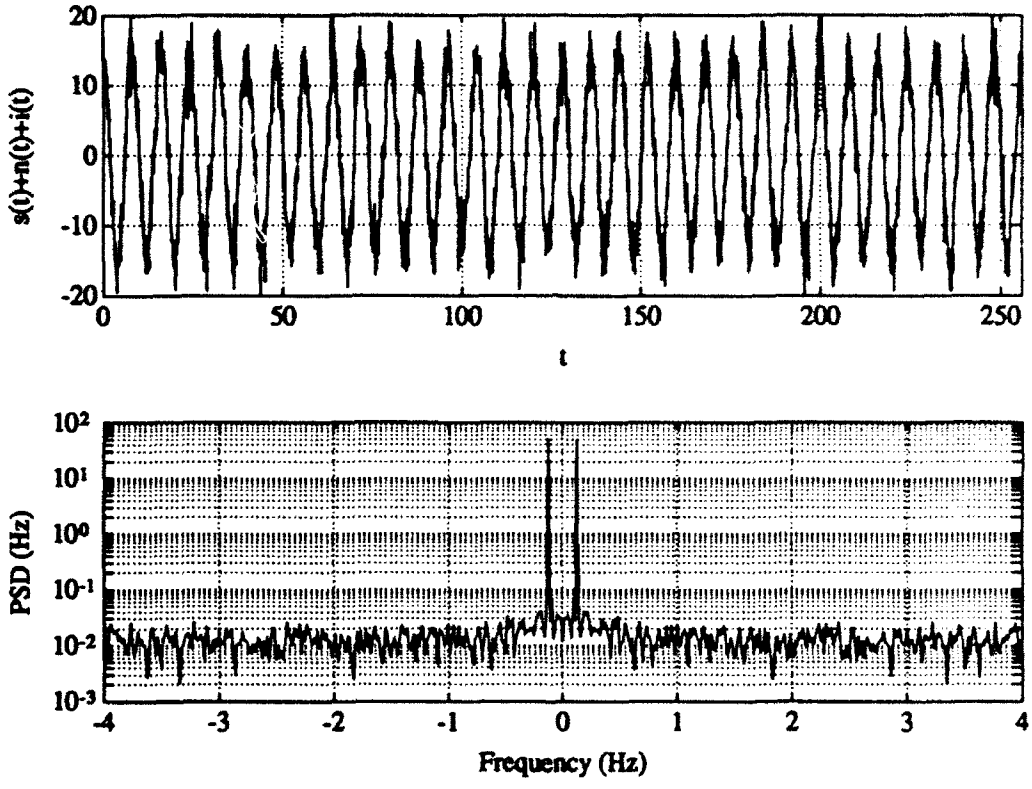

Figure 6: An example of the spread signal plus noise plus single-tone interference, and its power spectrum, $E_c/N_0 = -3.05$ dB (i.e., $E_b/N_0 = 12$ dB), $I/S = 20$ dB.

rectangular chips considered here, the matched filter can be implemented as an integrate-and-dump circuit operating at the chip rate. The output of the sampler is defined as

$$r_n = s_n + n_n + i_n \tag{1}$$

where s_n is the signal of amplitude $\pm E_c = 1$, n_n is white Gaussian noise of variance $N_0/2$, and i_n is a sample of interference.

Under normal conditions (i.e., no interference present), the sequence r_n in Fig. 1 would be applied to the PN correlator, which despreads the signal, followed by a discrete form of an integrate-and-dump system operating at the bit rate, and finally a bit detector. The output of the bit detector is represented as $\hat{D}_k$, which is an estimate of the k^{th} transmitted bit. It should be noted that the model of the receiver is an ideal one, in that perfect synchronization is assumed in the different parts of the system, i.e., the two samplers operate at the chip and bit rates, sampling the signals at the proper instants in time, and the PN correlator is in-phase with the received spread spectrum signal.

A few figures will now be presented for different points in the receiver to illustrate some of the above characteristics of the system.

For example, Fig. 7 illustrates two successive spread bits (32 chips/bit) taken at the output of the matched filter (no noise and interference added). Figure 8 shows the same two spread bits from Fig. 7 but with noise added ($E_c/N_0 = -3.05$ dB). Figure 9 illustrates these spread bits when interference is present. The effect of the interference on the received sequence is quite obvious. Figure 10 shows a sequence of 32 information bits D_k detected for infinite signal-to-noise-plus-interference ratio conditions (upper graph) and the same 32 bits at the output of the bit detector, $\hat{D}_k$ when noise and interference are present (lower graph). Comparing the upper and lower frames in this figure shows a number of bit errors in the lower frame. Finally, Fig. 11 illustrates the effect of suppressing the interference with the FFT-based suppression filter which will be described in the next section. Comparing the upper and lower frames shows that the bit errors have disappeared (at least for this group of bits).

4.0 INTERFERENCE SUPPRESSION ALGORITHM

This section will describe the essence of the FFT-based suppression algorithm as outlined in [1], with elaborations as required.

The basis for the FFT method is that the power density spectrum of the PN sequence is relatively flat while the spectrum of the narrow-band interference is highly peaked. This is particularly true for the sampled signal at the output of the matched

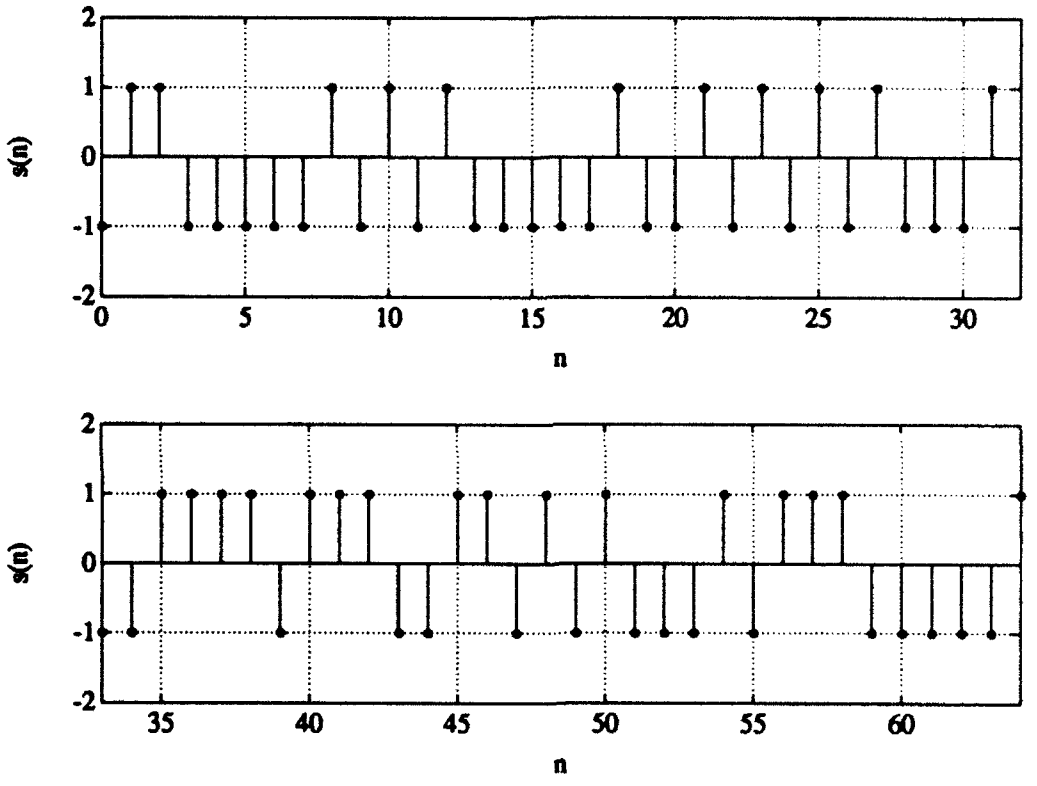

Figure 7: An example of two successive spread bits at the output of the matched filter in Fig. 1.

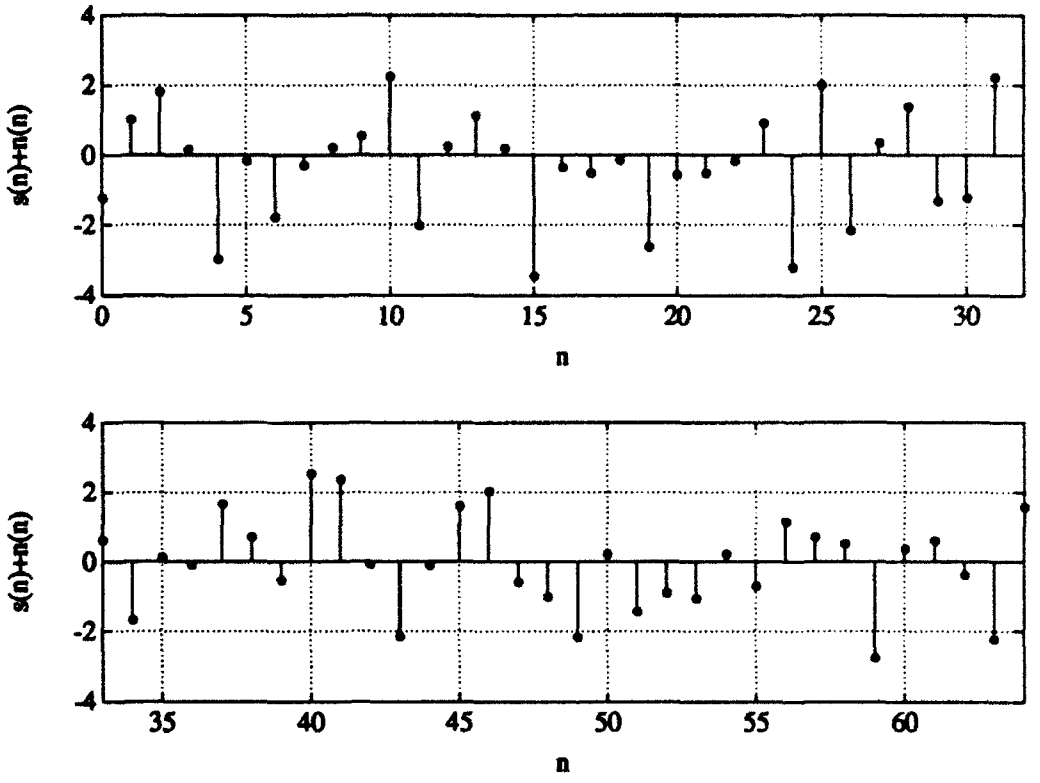

Figure 8: An example of the spread signal in Fig. 7 plus noise at the output of the matched filter in Fig. 1 for the case of $E_b/N_0 = 12$ dB, $E_b = 32$ units.

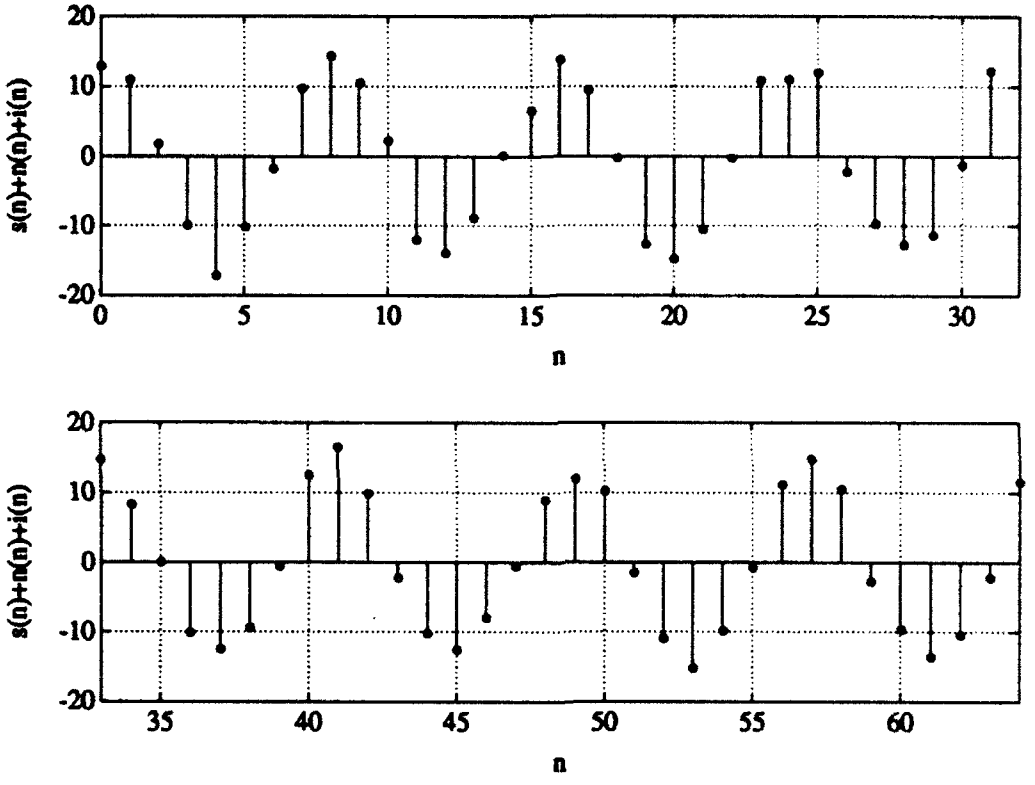

Figure 9: An example of the spread signal in Fig. 7 plus noise and interference at the output of the matched filter in Fig. 1 for the case of $E_b/N_0 = 12$ dB, $E_b = 32$ units, and interference-to-signal ratio of 20 dB.

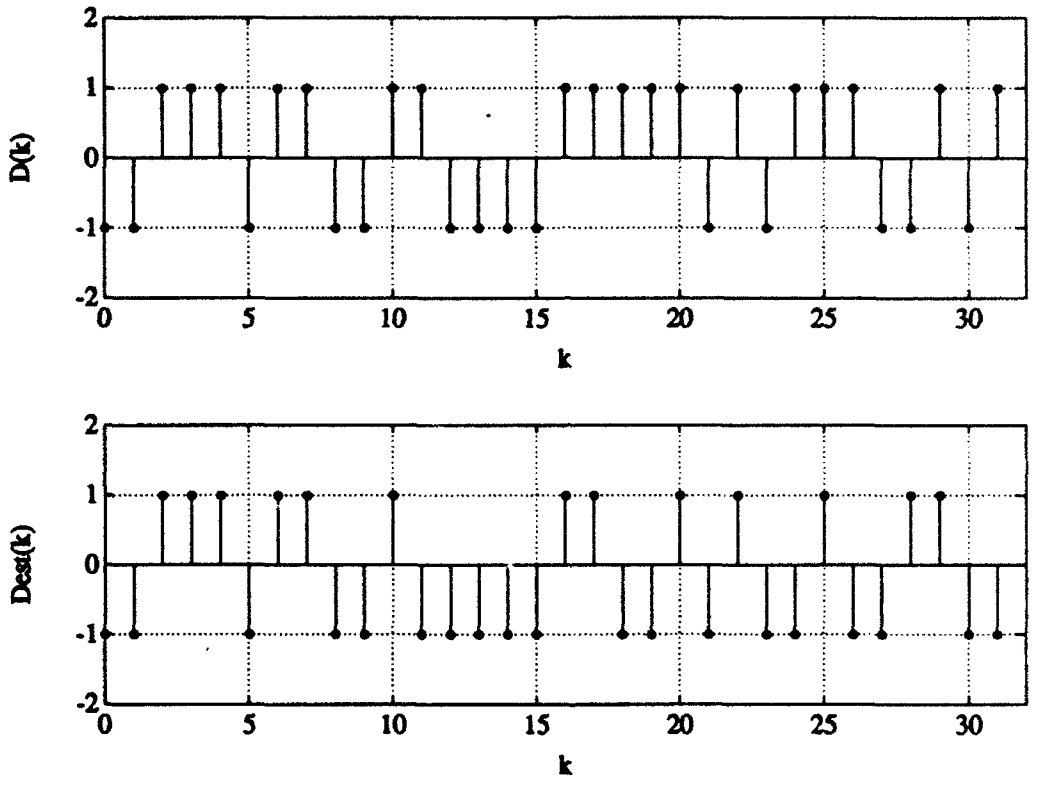

Figure 10: An example of 32 bits at the output of the bit detector when no noise or interference is present (upper graph), and when noise and interference are present (lower graph); notice that there are several bit errors. For the noise and interference case, $E_b/N_0 = 12$ dB, $E_b = 32$ units, and interference-to-signal ratio of 20 dB.

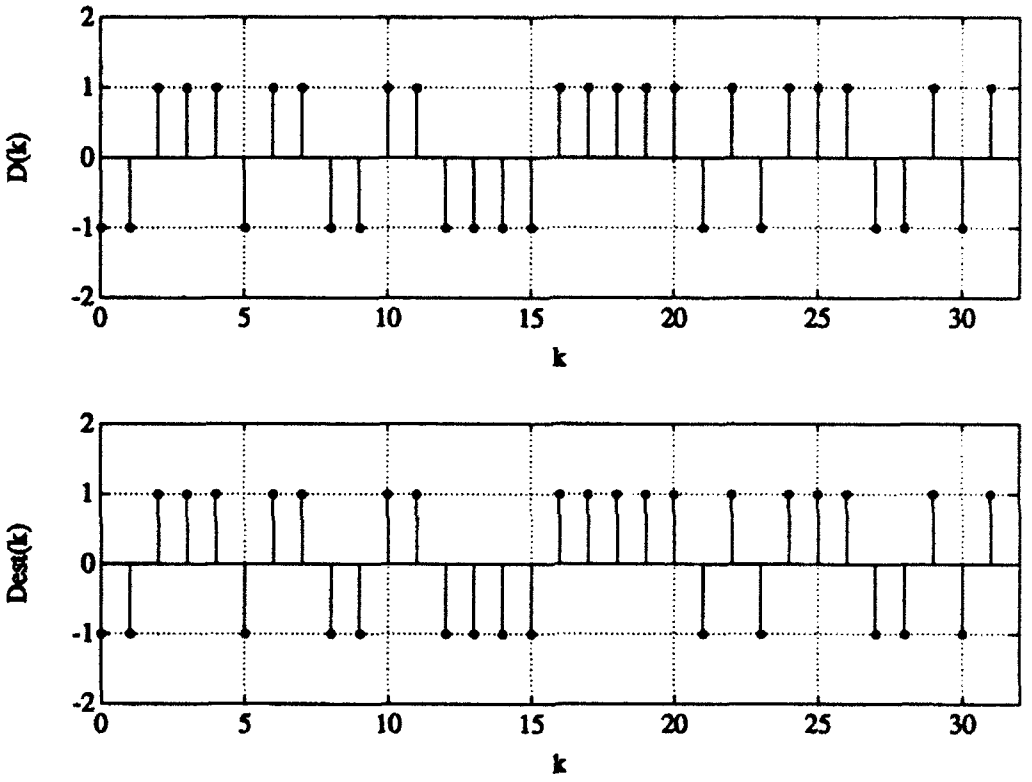

Figure 11: An example (with the interference suppressor present) of 32 bits at the output of the bit detector when no noise or interference is present (upper graph), and when noise and interference are present (lower graph); notice that there are no bit errors. For the noise and interference case, $E_b/N_0 = 12$ dB, $E_b = 32$ units, and interference-to-signal ratio I/S of 20 dB.

filter in Fig. 1. There, each signal sample (chip) of s_n can be viewed as being independent of other signal samples, resulting in a "white-noise" signal sequence, whereas each interference sample, because it is narrow-band, is highly correlated with past and future interference samples.

The first step in this method is to estimate the power spectral density of the received signal r_n as represented by Eq. (1). The spectral estimate can be obtained by the Welch method [3].

Once the PSD of the received signal is estimated for a given block of data, the interference suppression filter can be designed for that block. A transversal filter is an appropriate structure for this application, since it is desired to use a filter that contains notches (zeroes) in the frequency range occupied by the interference. A method for designing the transversal filter in the discrete-time domain is to select its discrete Fourier transform (DFT) to be the reciprocal of the square root of the power spectral density at equally spaced frequencies.

To elaborate, suppose that the transversal filter has N taps. Since it is not desired to have a notch at 0 or π radians, a Type 1 filter (N odd, and symmetric impulse response) will be required. The problem is to specify the N tap coefficients $\{h(n)\}$ or equivalently, its DFT, $H(k)$, defined as

$$H(k) = \sum_{n=0}^{N-1} h(n) e^{-j\frac{2\pi}{N}nk}, \quad k = 0, 1, ..., N-1. \tag{2}$$

In terms of the PSD of the received signal, $H(k)$ is given by

$$H(k) = \frac{1}{\sqrt{P(k/N)}} e^{-j\frac{2\pi}{N}(\frac{N-1}{2})k} \tag{3}$$

where $P(f)$, defined for $0 \leq f \leq 1$, denotes the estimate of the PSD. Note that $P(f)$ is periodic with period 1 Hz; the folding frequency is 1/2 Hz. For a linear phase filter, the impulse response $h(n)$ must be symmetric (i.e., $h(n) = h(N-1-n)$).[6]

Since the FFT algorithm produces a spectrum consisting of an even number of values and an odd number of taps are required, an interpolation algorithm operating on the given PSD samples from the Welch algorithm must be carried out. For example, if an N—tap filter is desired (N=15, say) and the power spectrum consists of M=16 or 32

[6] As noted earlier, [1] considered a BPSK spread spectrum signal. For, say, a QPSK type of spread spectrum signal, the condition to be satisfied would be $h(n) = h^*(N-1-n)$, where * denotes complex conjugate.

samples at frequencies 0 to $(M-1)/M$ Hz in steps of $1/M$ Hz, values for $P(k/N)$ in Eq. (3) would have to be obtained at equally spaced intervals over the range 0 to $(N-1)/N$ Hz in intervals of $1/N$ Hz.

The steps taken to calculate a set of filter coefficients $\{h(n)\}$ for the suppression filter are as follows:

(1.0) obtain a block of data from r_n, the output of the matched filter in Fig. 1

(2.0) calculate the power spectrum using the Welch algorithm for a pre-defined sub-block size M, overlap size S, and window function (rectangular, Hanning, etc.)

(3.0) the previous step yields $P(k/M)$, $k = 0, 1, \cdots, (M-1)$

(4.0) interpolate [7] this function at the new set of frequencies, $k = 0, 1, \cdots, (N-1)$, resulting in the desired samples $\sqrt{P(k/N)}$, $k = 0, 1, \cdots, (N-1)$

(5.0) calculate the function $1/\sqrt{P(k/N)}$, $k = 0, 1, \cdots, (N-1)$

(6.0) calculate the DFT, $H(k)$, from Eq. (3)

(7.0) calculate the filter coefficients $h(n)$ of the suppression filter

(8.0) apply the block of data collected in step 1 to the filter.

After the block of data has been filtered, the output of the suppression filter, e_n in Fig. 1, is applied to the PN correlator. It should be noted that, because of a group delay of $(N-1)/2$ samples caused by the suppression filter, the PN correlator must be delayed by this amount as well.

5.0 SIMULATION RESULTS

This section presents several results illustrating the steps for calculating the tap coefficients of the suppression filter, and some examples for different interference conditions.

[7] A cubic spline interpolator was used, although other, more simple interpolation techniques would be just as valid. The important issues to consider would be the relative performance trade-offs afforded by the different interpolation schemes versus their computational complexities.

5.1 SINGLE-TONE INTERFERENCE

Figure 12 shows the power spectrum of a single tone interferer (no signal or noise present), with power $P_i = 100$ (i.e., $I/S = 20$ dB as noted earlier) and frequency $f_i = 2/16$ Hz. The overall block size was 1024 points, the sub-block size was $M = 16$, and there was no overlapping of the sub-blocks ($S = 16$); a rectangular window was used so that a pure spectral line would be obtained in the power spectrum. In Fig. 12, two spectral lines of height 50 each (thus totalling the power of the interference) are obtained, thus verifying proper operation of the PSD estimator.

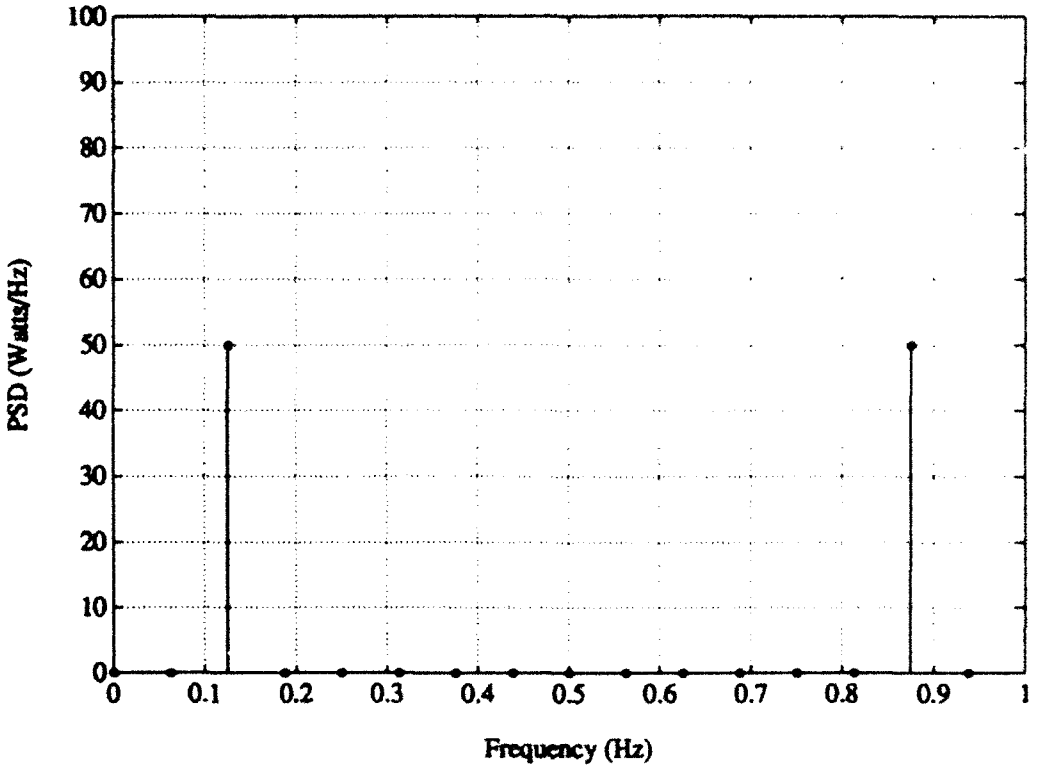

Figure 12: Power spectral density of an interferer located at 2/16 Hz, based on averaging 16-point sub-block FFT's from an overall block size of 1024 samples, and rectangular window weighting.

Figure 13 shows the PSD of r_n (signal, noise, and interference) calculated from a block of 1024 data samples at the output of the matched filter in Fig. 1. The interference-to-signal ratio/chip is 20 dB and $E_b/N_0 = 12$ dB with $E_b = L = 32$ units. Because of the high I/S condition, observe that the effect of the addition of signal and noise is hardly noticeable (upper spectrum). To show the contribution of the signal and noise to the power spectrum, a magnified version of the upper frame is illustrated in the lower frame.

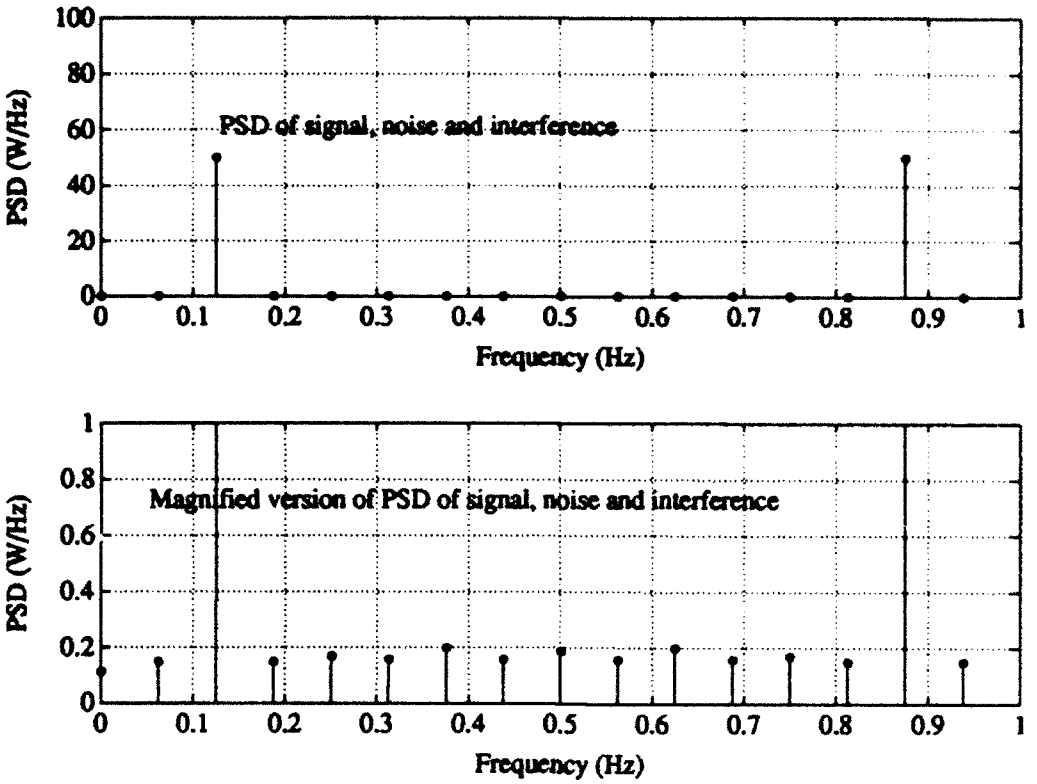

Figure 13: Power spectral density of signal, noise and interference located at 2/16 Hz (0.125 Hz), based on averaging 16-point sub-block FFT's from an overall block size of 1024 samples, and no weighting (i.e., rectangular window). The interference-to-signal ratio/chip is 20 dB and $E_b/N_0 = 12$ dB with $E_b = 32$ units. Because of the high I/S condition, observe that the effect of the addition of signal and noise is hardly noticeable (upper spectrum) compared to Fig. 12.

Figures 14, 15, and 16 illustrate, respectively, the square-root of the PSD (i.e., $\sqrt{P(k/M)}$, $k = 0, 1, \cdots, (M-1)$, $M = 16$), the interpolated spectrum (i.e., $\sqrt{P(k/N)}$, $k = 0, 1, \cdots, (N-1)$, $N = 15$), and the reciprocal of the interpolated spectrum (i.e., $1/\sqrt{P(k/N)}$, $k = 0, 1, \cdots, (N-1)$). Observe that the interpolated spectrum in Fig. 15 has changed slightly from the original one in Fig. 14, as expected. Finally, the reciprocal spectrum in Fig. 16 shows a very low level spectral line near the interference frequency 0.125 Hz, i.e., the desired notch frequency.

Figures 17 and 18 show, respectively, the magnitude and phase of $H(k)$ from Eq. (3). The magnitude is, as expected, the same as the spectrum in Fig. 16, and the phase in Fig. 18 is linear.

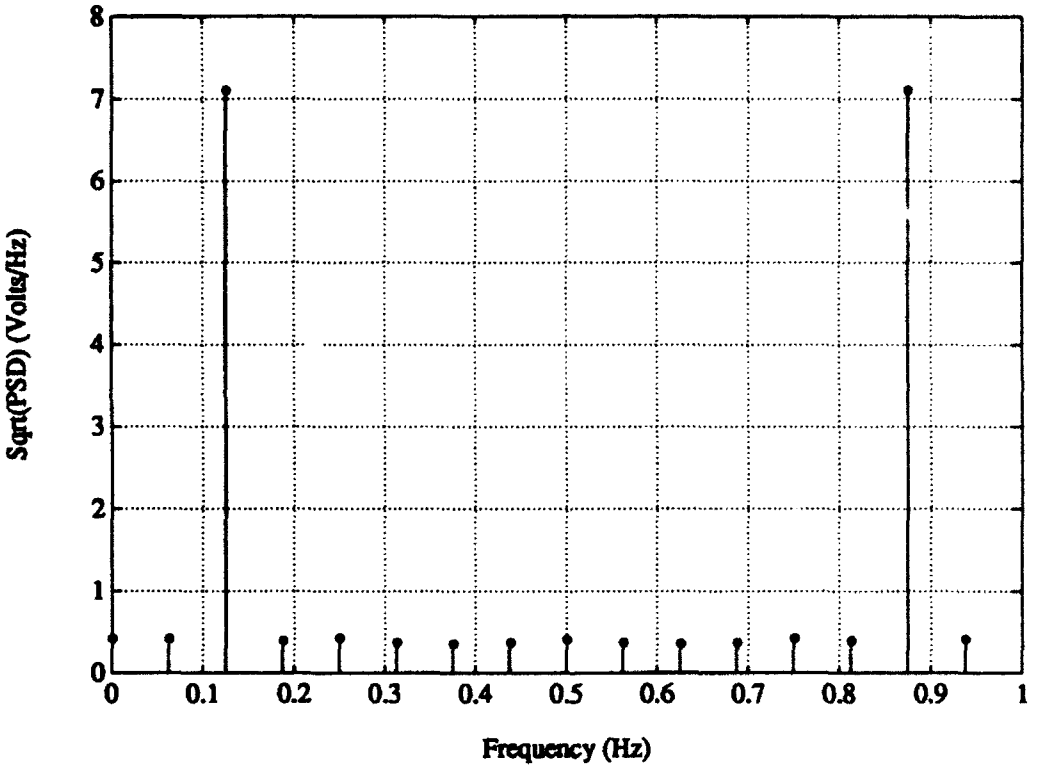

Figure 14: The square root of the power spectral density in Fig. 13.

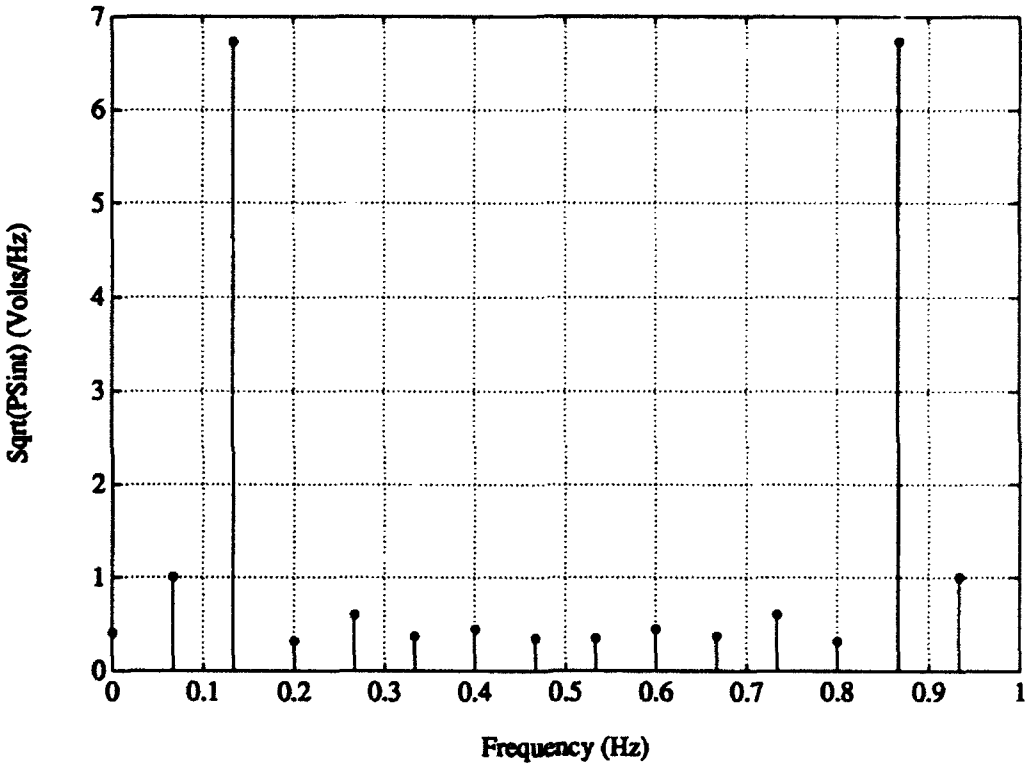

Figure 15: The square root of the interpolated power spectral density of signal, noise and interference, obtained by interpolating the spectrum in Fig. 14.

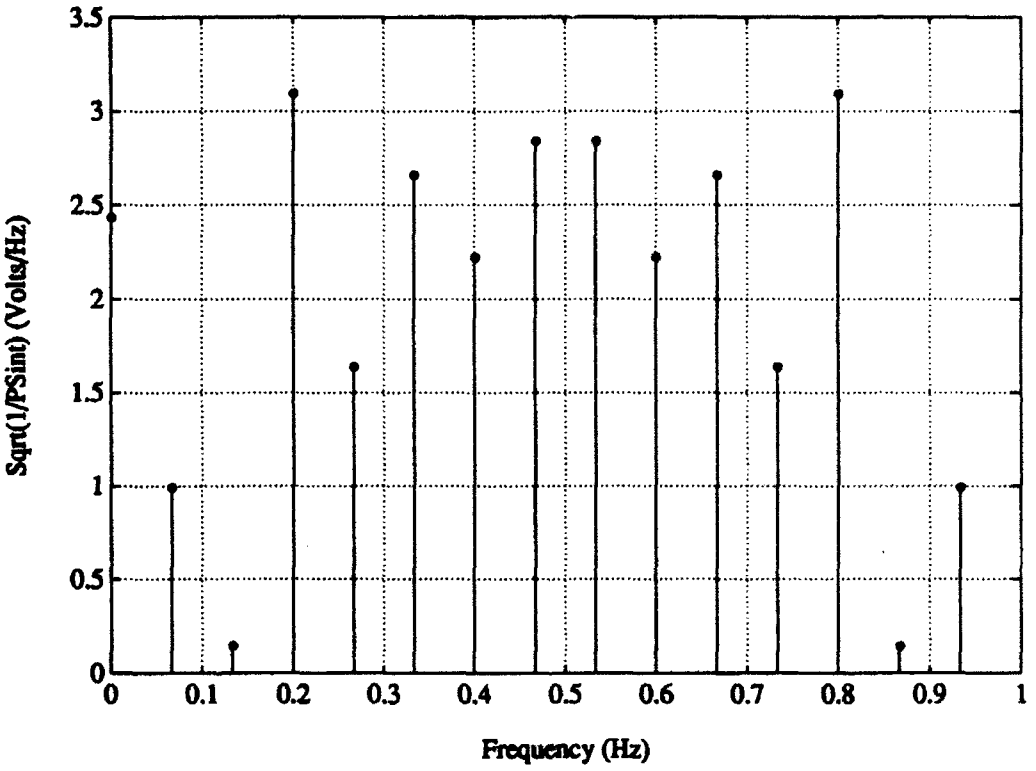

Figure 16: The reciprocal of the spectrum in Fig. 15.

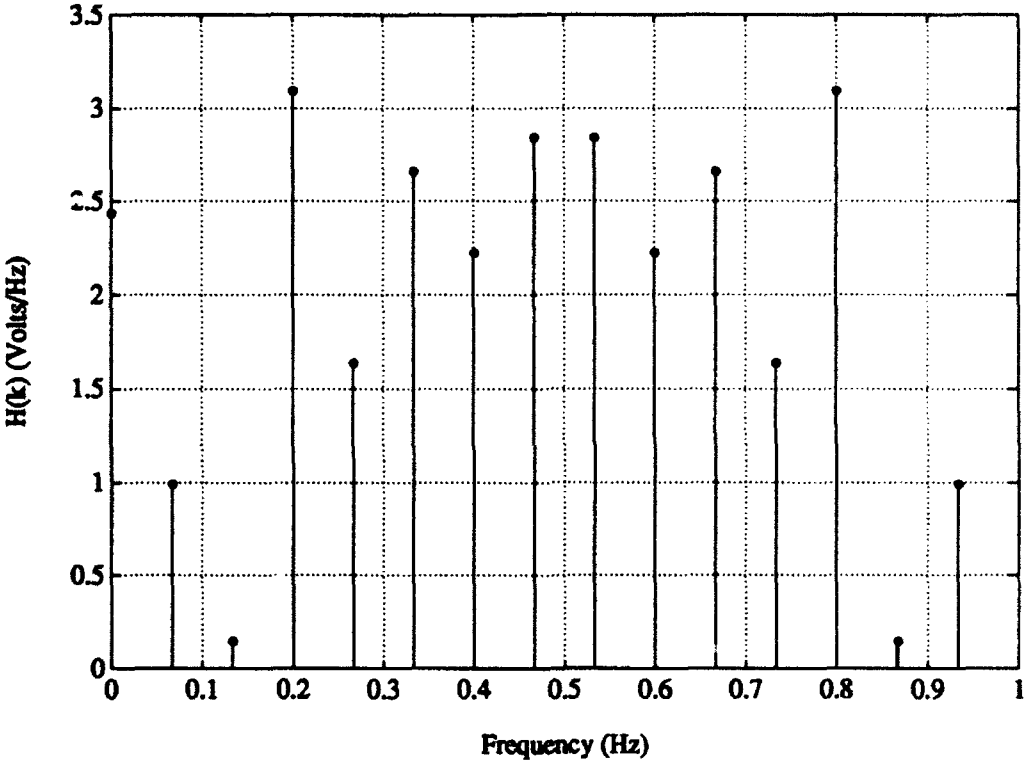

Figure 17: The magnitude of the transfer function $H(k)$ of the interference suppression filter; the magnitude is equivalent to the spectrum in Fig. 16.

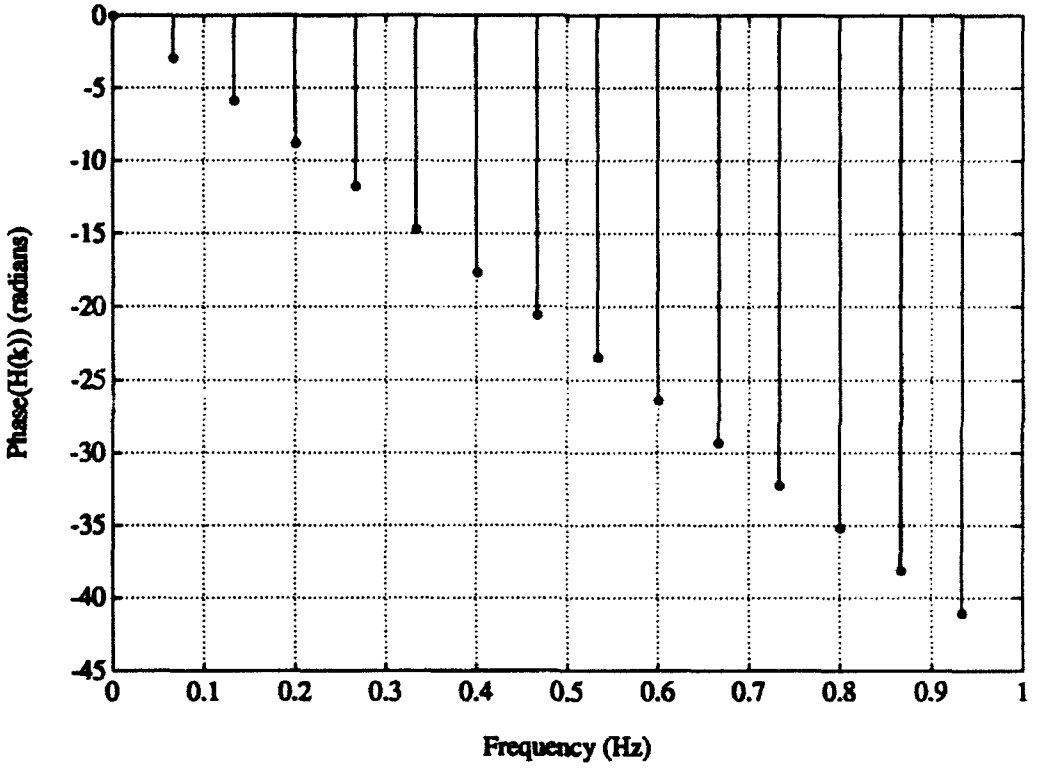

Figure 18: The phase $\phi(k)$ of the interference suppression filter with transfer function $H(k)$.

Figures 19 and 20 respectively illustrate the unnormalized filter coefficients $h(n)$ (obtained from the inverse DFT applied to $H(k)$) and normalized filter coefficients (obtained by dividing each tap $h(n)$ by the weight of the center tap). The normalized set of coefficients is useful when one wishes to compare the original sequence r_n from Eq. (1) with its filtered counterpart e_n. If normalization of the filtered sequence is not done, and it is desired to carry out a comparison between the output and input of the suppression filter, one would have to keep track of the gain from block-to-block and multiply r_n by this gain factor.

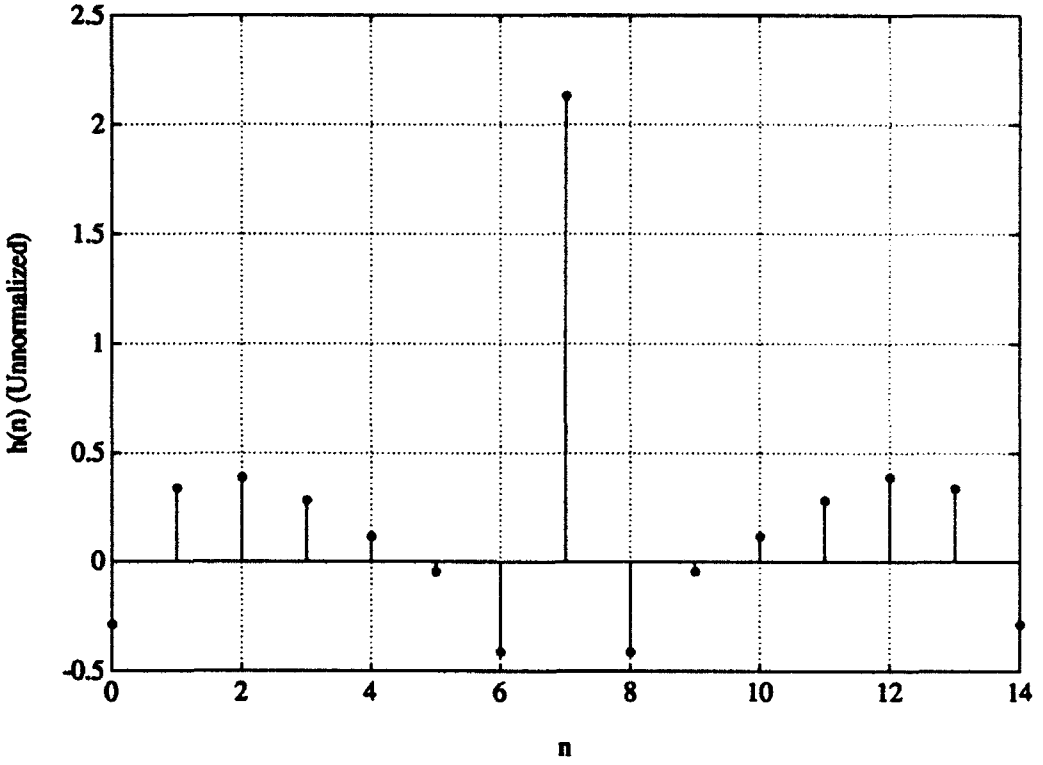

Figure 19: The impulse response $h(n)$ of the suppression filter, $H(k)$.

Figure 21 illustrates the magnitude of the continuous transfer function of the designed suppression filter using the normalized set of tap weights from Fig. 20. As the figure indicates, strong suppression is achieved in the neighbourhood of the tone frequency of 0.125 Hz and in the region around it. One would therefore expect to obtain approximately 20 to 25 dB suppression of the interference. In fact, Fig. 22 shows the power spectrum of r_n before the suppression filter (upper frame) and the power spectrum of e_n after the filter (lower frame), both calculated for the 1024 sample block used in estimating the coefficients of the suppression filter. In calculating these PSD's, the 1024

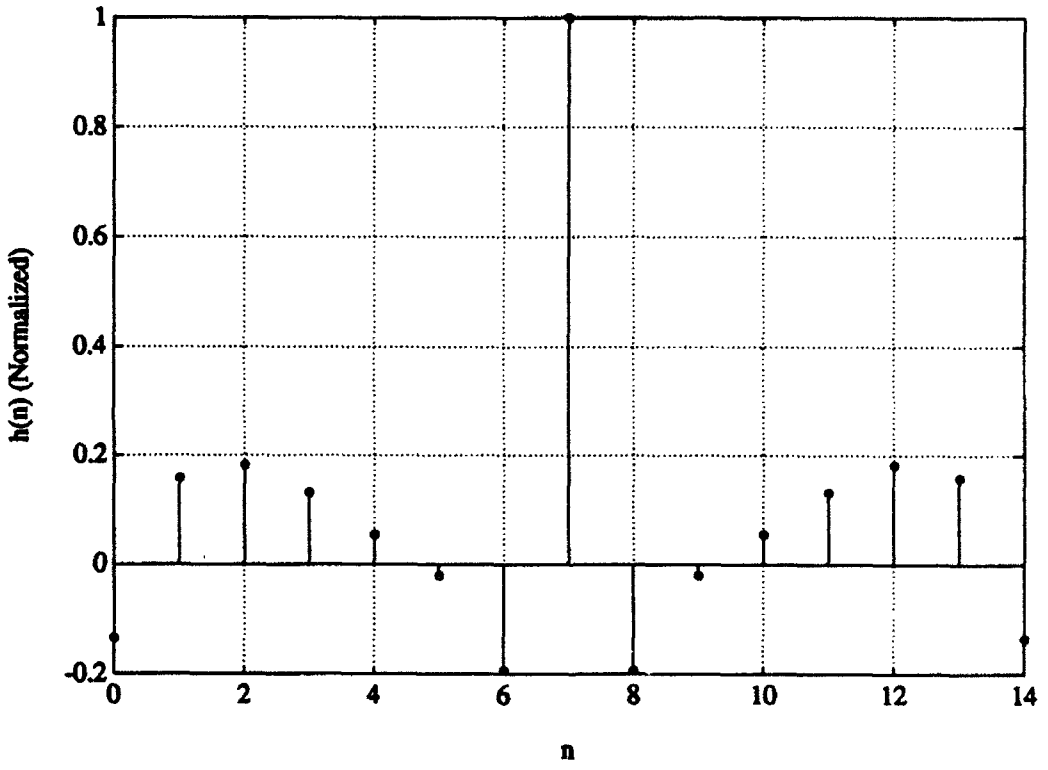

Figure 20: The normalized impulse response $h(n)$ of the linear suppression filter, $H(k)$.

samples were used with sub-blocks of 256 samples and no overlapping. Comparing the upper and lower spectra, one can see that the tone has been suppressed by about 20 dB, and that there is some rippling in the output spectrum caused by the suppression filter.

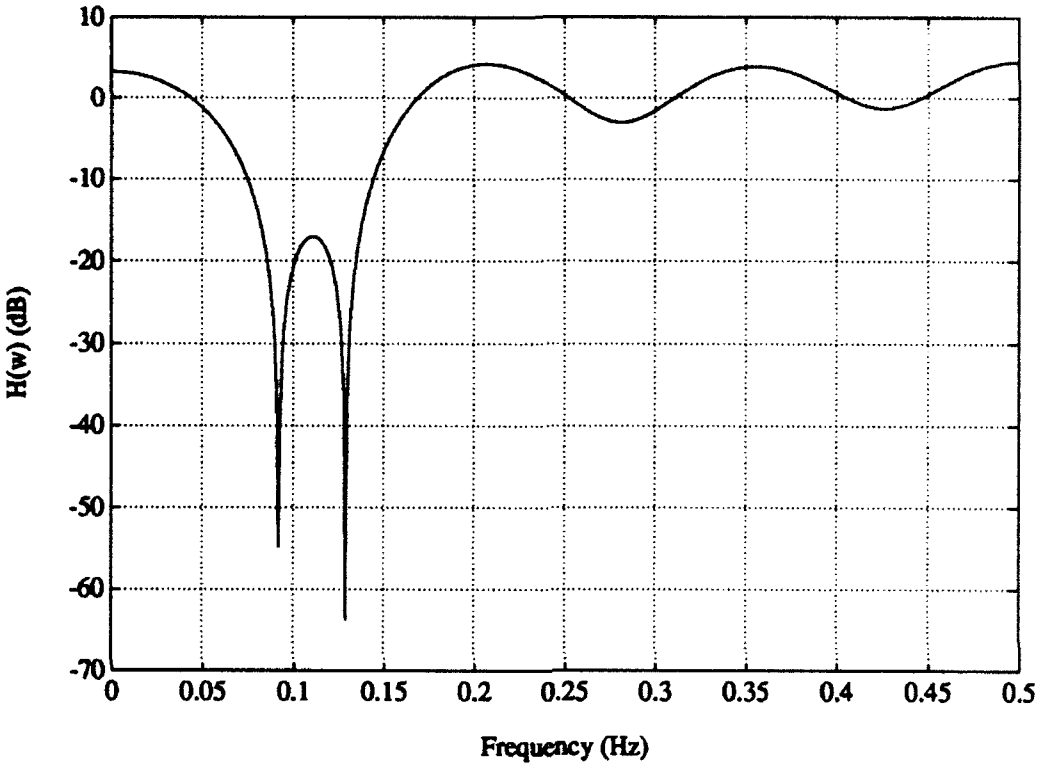

Figure 21: The continuous spectrum, $H(e^{j\omega})$, of the interference suppression filter with impulse response $h(n)$ calculated for $E_b/N_0 = 12$ dB, and tone frequency $f_i = 0.125$ Hz.

The bit error rate performance is considered next. To obtain this performance, the simulation conditions were initially set up as follows:

- interference-to-signal ratio equal to 20 dB
- E_b/N_0 ranged from 0 to 12 dB
- processing gain L was set to 32
- filter order N=15
- 1024 points/block, sub-block size M=16, no-overlapping, and rectangular window
- tone frequency $f_i = 2/16$ Hz

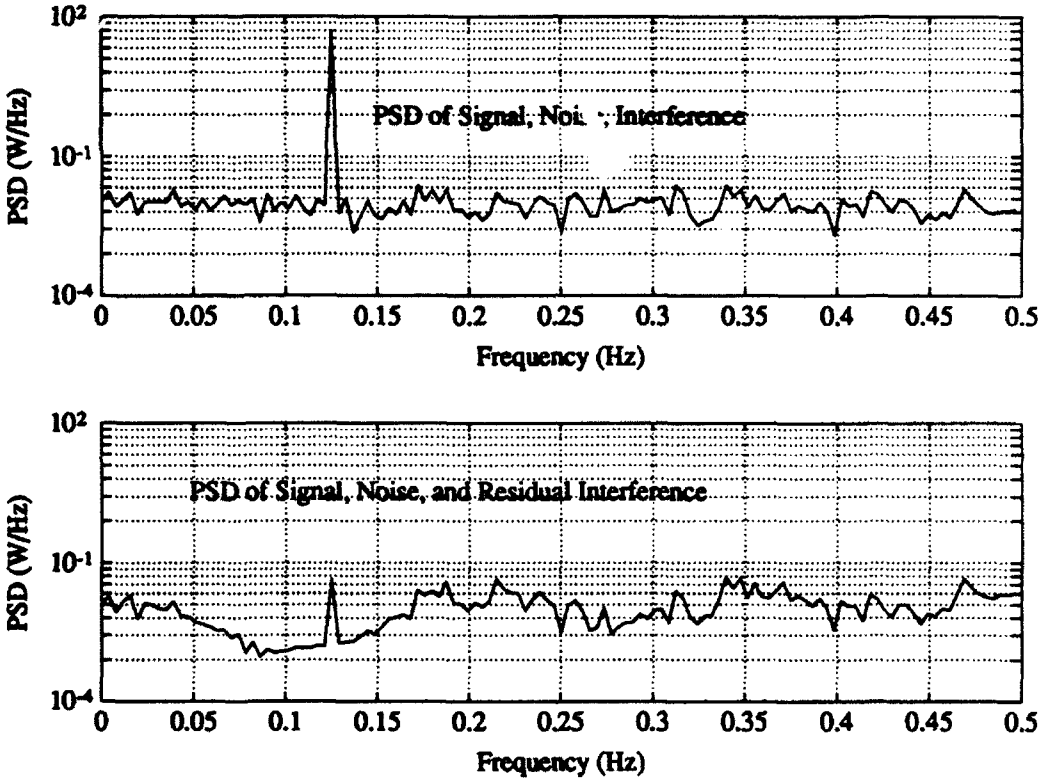

Figure 22: The power spectra of r_n (upper frame) before the suppression filter, and e_n (lower frame) after the suppression filter for the block of 1024 samples used to calculate the filter coefficients h_n in Fig. 20.

- number of bits transmitted when suppression filter not present, 10,000
- number of bits transmitted when suppression filter present, 100,000[8].

The results of this test are illustrated in Fig. 23. When the suppression filter was not present, the bit error rate was close to 0.5 for all E_b/N_0's considered. With the suppression filter present the performance improves significantly, until it levels off at near 11 to 12 dB, indicating that an irreducible error has been arrived at for this particular case. Notice that there is a strange hump in the bit error rate curve appearing between $E_b/N_0 = 2$ and 5 dB. This feature did not disappear for different random number seeds. On closer analysis of this problem, it was found that it was a function of the frequency being at exactly 2/16 Hz. An example of the magnitude of $H(e^{j\omega})$ is illustrated in Fig. 24 for $E_b/N_0 = 4$ dB. Even though a notch is located at the desired frequency, there are several others, including a significant amount of noise amplification at $f = 0.2$ Hz. This effect disappeared when a Hanning window was used. The magnitude of the transfer function $H(e^{j\omega})$ for this latter case is illustrated in Fig. 25, and the corresponding bit error rate curve is shown in Fig. 26.

When the frequency was changed to a spectrally unrelated value, and with rectangular weighting, the problem also disappeared. The bit error rate curve for a tone located at $f_i = 0.1111$ Hz is illustrated in Fig. 27.

5.2 HOPPING-TONE INTERFERENCE

For this example, a single-tone, hopping between two frequencies was considered. The frequencies selected were $f_0 = 0.1111$ Hz and $f_1 = 0.3111$ Hz. The hopping rate was selected such that the frequency changed from f_0 to f_1 every 10 blocks. A 3—D plot illustrating the adaptive nature of the suppression filter is shown in Fig. 28. It should be noted that the Hanning window was used here, the rectangular one producing inferior results for the interference at frequency $f_1 = 0.3111$.

The bit error rate performance for this case is shown in Fig. 29. Observe that the performance is worse than that for the stable tone. There are two reasons for this. The first is that the degree of interference suppression is a function of the tone's frequency offset from the spread spectrum carrier [4]. The second is that the bandwidth of the notch appeared to be much larger for the frequency $f_1 = 0.31111$ Hz compared to $f_0 = 0.1111$ Hz.

[8]The number of bits transmitted was increased by a factor of 10 so as to obtain reasonable statistical results on one run when the suppression filter was present.

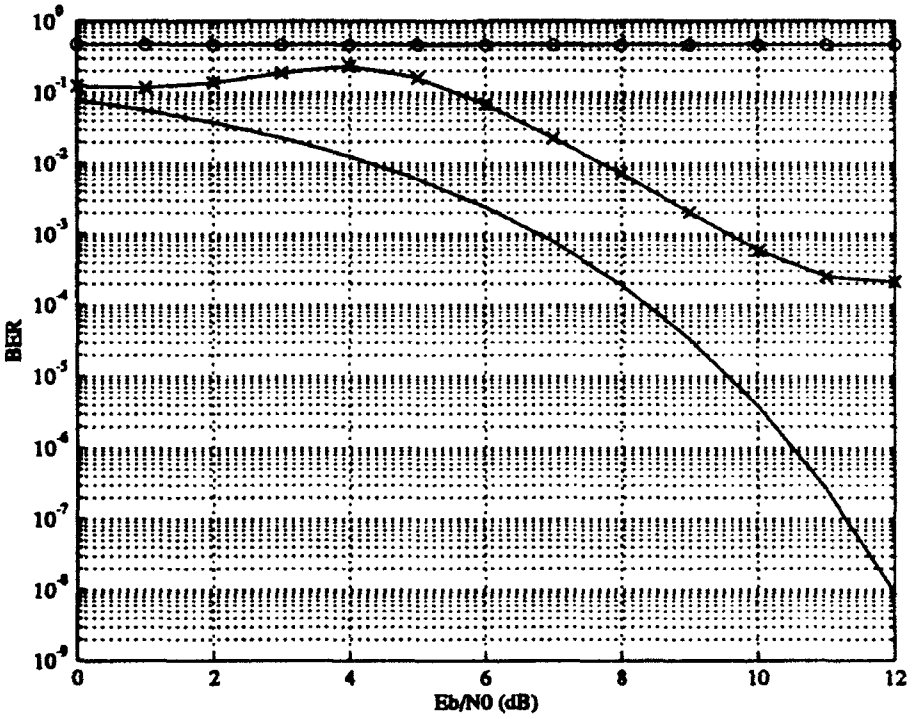

Figure 23: Bit error rate performance for a single tone interferer at frequency $f_i = 2/16$ Hz without the suppression filter ('o') and with the suppression filter ('x'). The solid curve ('—') corresponds to the theoretical bit error rate for a signal in additive white Gaussian noise.

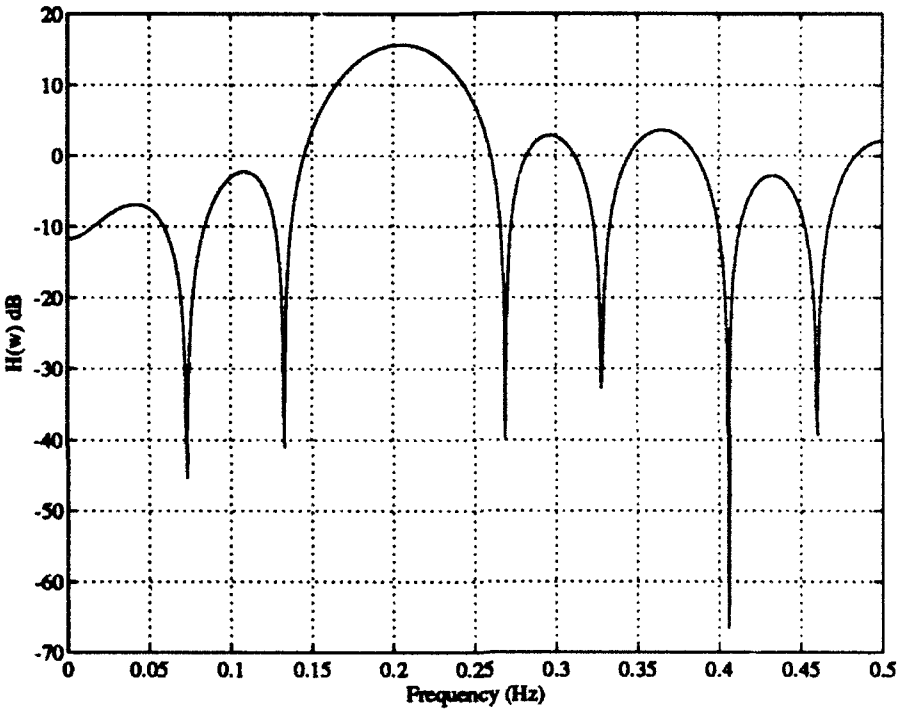

Figure 24: The continuous spectrum, $H(e^{j\omega})$, of the interference suppression filter with impulse response $h(n)$ calculated for $E_b/N_0 = 4$ dB, and tone frequency $f_i = 0.125$ Hz. A rectangular window was used in estimating the filter coefficients.

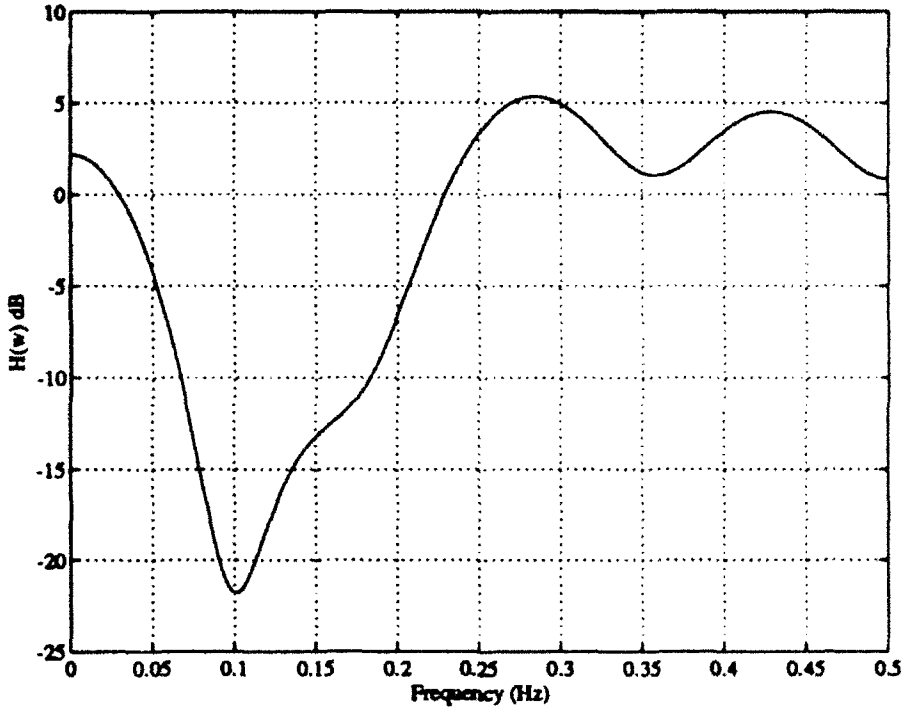

Figure 25: The continuous spectrum, $H(e^{j\omega})$, of the interference suppression filter with impulse response $h(n)$ calculated for $E_b/N_0 = 4$ dB, and tone frequency $f_i = 0.125$ Hz. A Hanning window was used in estimating the filter coefficients.

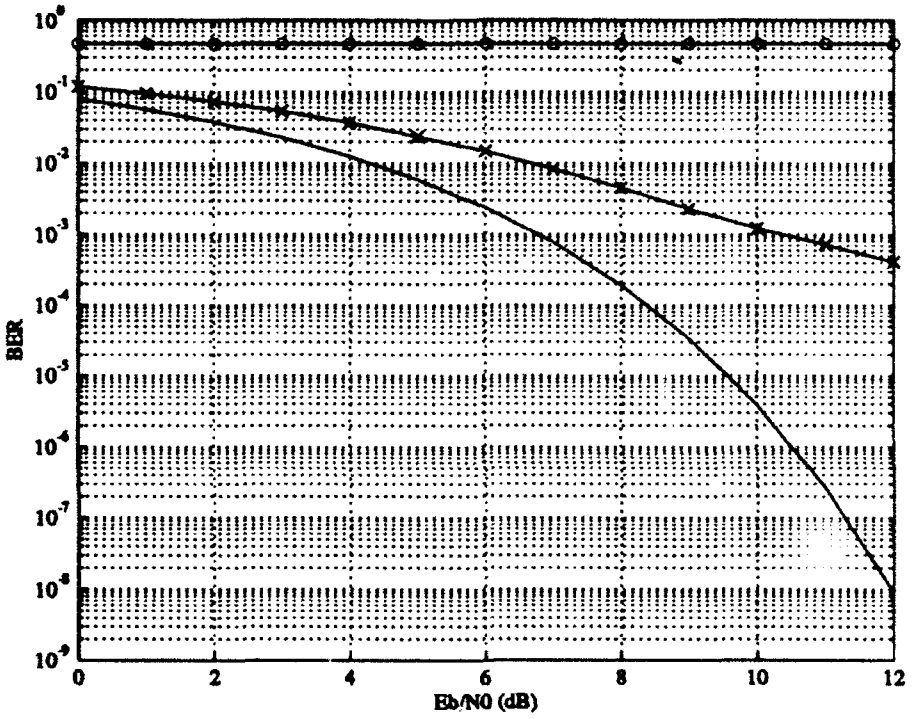

Figure 26: Bit error rate perfcrmance for a single tone interferer at frequency $f_i = 0.125$ Hz without the suppression filter ('o') and with the suppression filter ('x'). The solid curve ('—') corresponds to the theoretical bit error for a signal in additive white Gaussian noise. A Hanning window was used in estimating the filter coefficients.

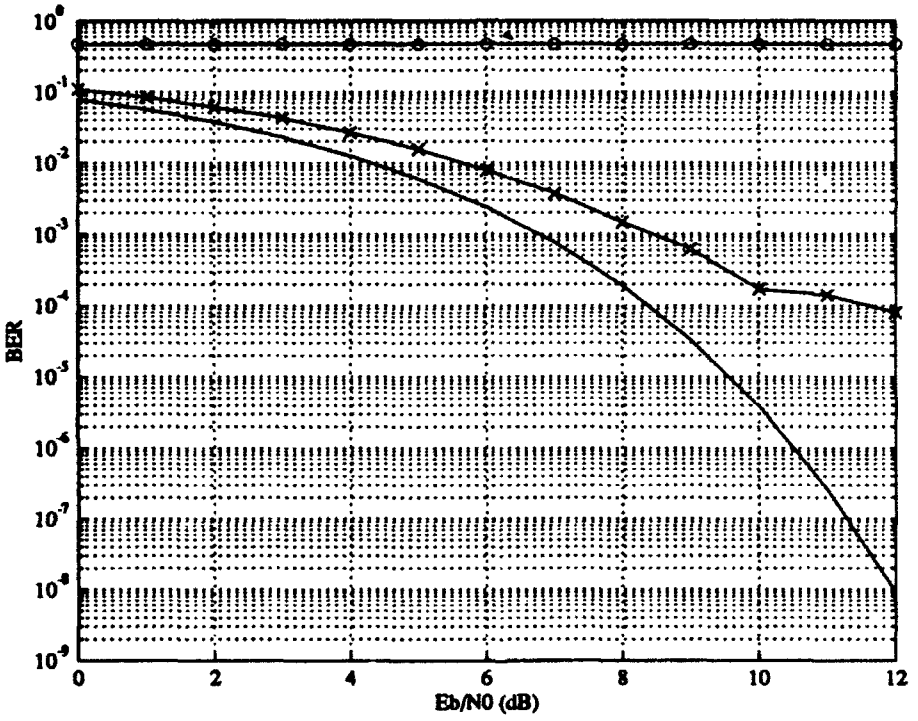

Figure 27: Bit error rate performance for a single tone interferer at frequency $f_i = 0.1111$ Hz without the suppression filter ('o') and with the suppression filter ('x'). The solid curve ('—') corresponds to the theoretical bit error for a signal in additive white Gaussian noise.

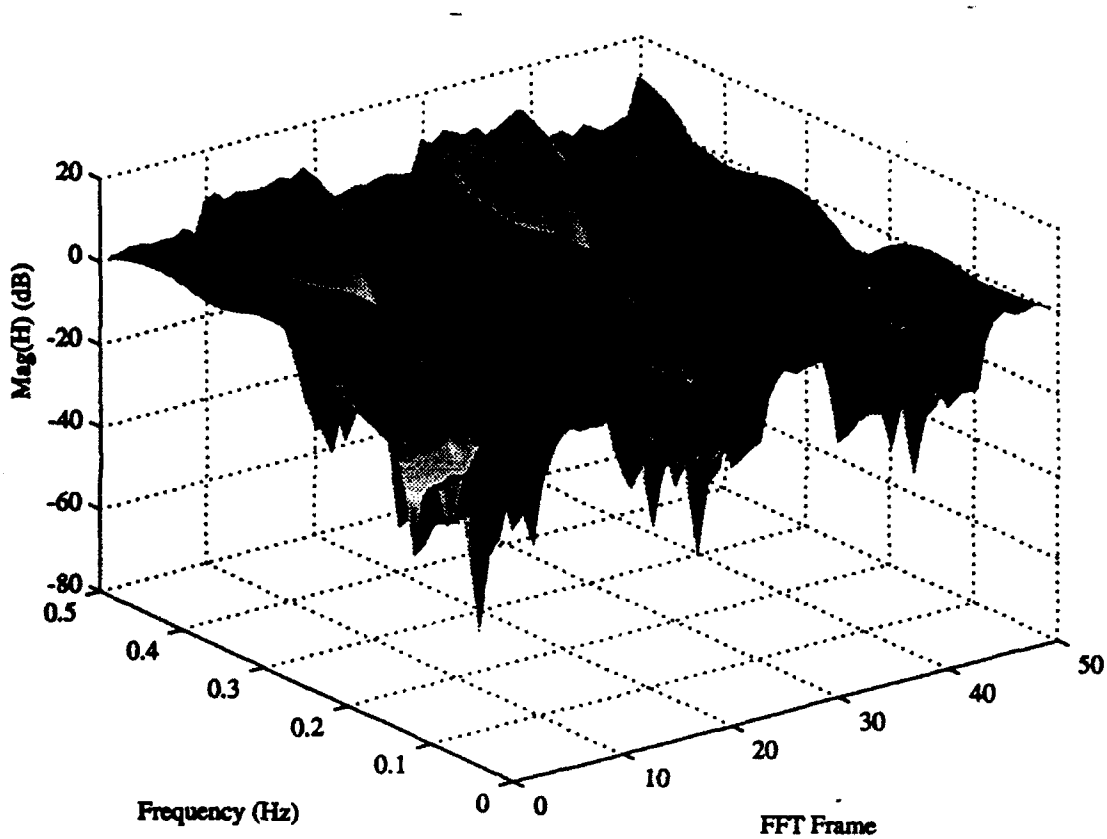

Figure 28: Three-dimensional view of the FFT-based adaptive suppression filter for a signal hopping between two frequencies.

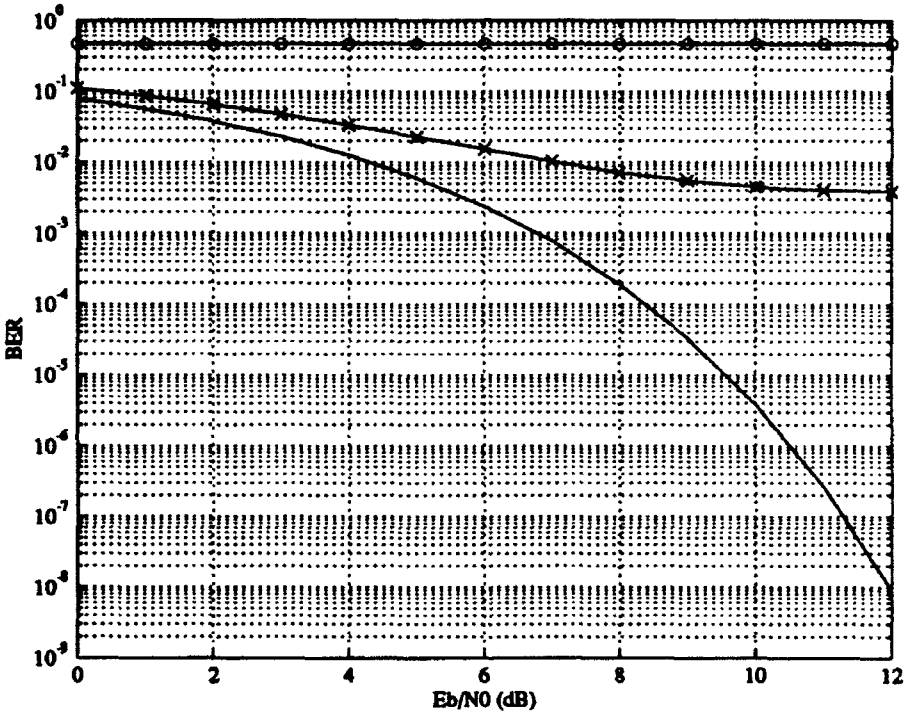

Figure 29: Bit error rate performance for a hopping tone interferer, with hopping frequencies $f_0 = 0.1111$ Hz and $f_1 = 0.31111$, without the suppression filter ('o') and with the suppression filter ('x'). The solid curve ('—') corresponds to the theoretical bit error for a signal in additive white Gaussian noise.

6.0 CONCLUDING REMARKS

This technical note has presented an adaptive algorithm based on the FFT approach for suppressing narrow-band interference. Certain problems appeared to occur with the rectangular window. The initial conclusion was that, in general, a non-rectangular window would be more appropriate to forestall any problems. However, upon closer examination, the problem seemed to be due to the interpolation portion of the algorithm.

To elaborate, there are two interpolation approaches one can take when attempting to determine the notch filter transfer function, $H(e^{j\omega})$. Given the power spectrum from the Welch algorithm obtained from a particular block of data, one can:

- carry out the interpolation on the square-root of this spectrum followed by calculation of the reciprocal of the result, or
- calculate the reciprocal first and then interpolate.

The first approach can produce some strange results as noted in the report; however, the notch filter appears to provide good suppression when it does work. The second approach does not appear to produce any strange results, but the degree of suppression is less than the first approach (refer to Figs. 30 and 31). More work in this area is required.

Other points must be borne in mind with respect to the interpolation algorithm. It is important that the interpolated power spectrum values be positive. In some cases it was found that some interpolated values could be negative. Under these conditions, the absolute value was taken. Finally, it would be interesting to examine other simpler (e.g., zero- or first-order hold) interpolation schemes to see what their effect would be.

It is suggested that the filter order be close to the size of the sub-block used in estimating the power spectrum. If the filter order is significantly less than the sub-block size, a shallow notch will result.

Improved performance can perhaps be achieved if larger sub-blocks are used, but this will be at the expense of a large filter order. To reduce the variance on the noise on the power spectrum estimate, however, one would have to increase the overall block size (i.e., the number of sub-blocks to be averaged). This may prove to be unacceptable in an interference environment that changes quickly. This is where the strength of the high-resolution techniques (i.e., the parametric algorithms) are most noticeable—filter coefficients can be estimated on short blocks and still achieve excellent performance. However, as mentioned in the introduction to this study, the computational requirements of the parametric algorithms can prove to be a drawback, especially for large order filters. This is due to the need to determine the autocorrelation function of the input signal, r_n,

followed by the calculation of a matrix inverse in order to solve for the filter coefficients.

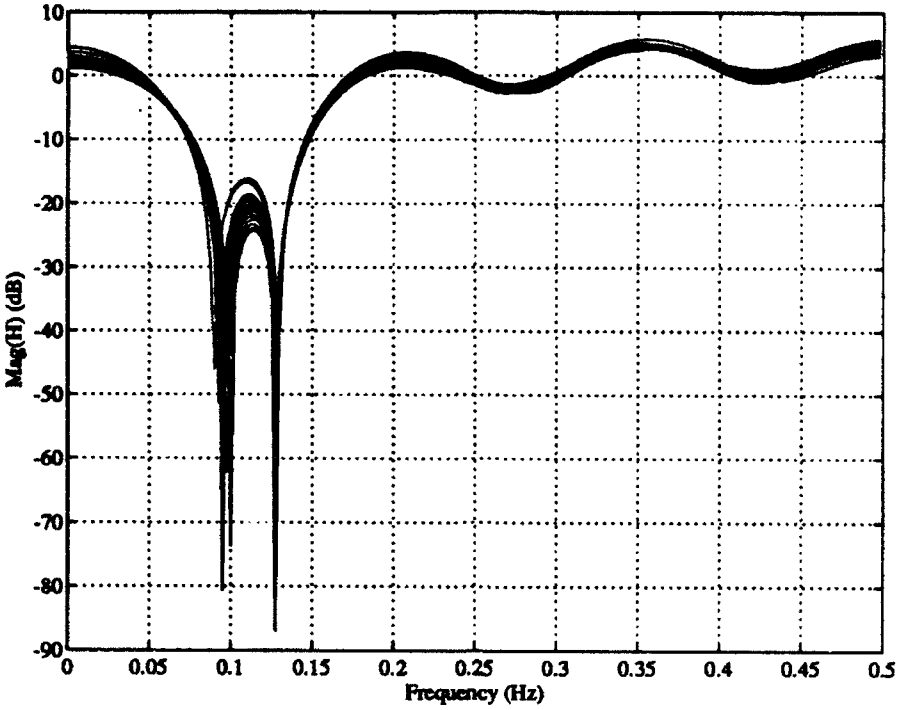

Figure 30: Thirty frames of the continuous spectrum, $H(e^{j\omega})$, of the interference suppression filter with impulse response $h(n)$ calculated for $E_b/N_0 = 12$ dB, and tone frequency $f_i = 0.125$ Hz. A rectangular window was used in estimating the filter coefficients. Interpolation was carried out on $\sqrt{P(k/M)}$, $k = 1, 2, \cdots, M-1$, $M = 16$.

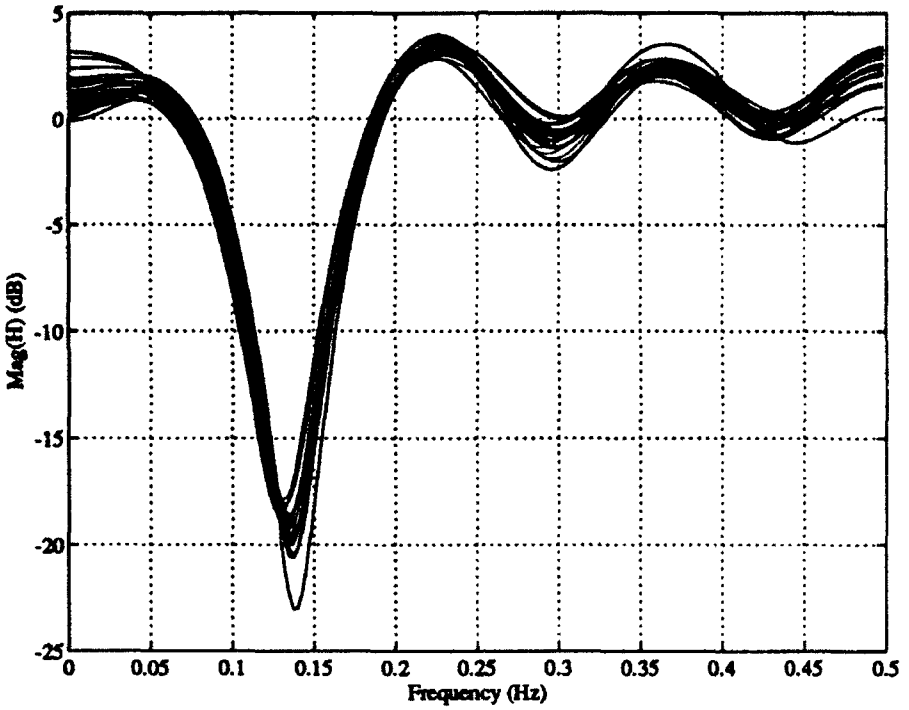

Figure 31: Thirty frames of the continuous spectrum, $H(e^{j\omega})$, of the interference suppression filter with impulse response $h(n)$ calculated for $E_b/N_0 = 12$ dB, and tone frequency $f_i = 0.125$ Hz. A rectangular window was used in estimating the filter coefficients. Interpolation was carried out on $1/\sqrt{P(k/M)}$, $k = 0, 1, 2, \cdots, M-1$, $M = 16$.

REFERENCES

[1] J. W. Ketchum and J. G. Proakis, "Adaptive algorithms for estimating and suppressing narrowband interference in PN spread-spectrum systems," *IEEE Transactions on Communications*, vol. 30, pp. 913–924, May 1982.

[2] D. Elsaesser and B. W. Kozminchuk, "Advanced communications ESM system (ACES) design considerations," Technical Note 92-2, Defence Research Establishment Ottawa, Ottawa, Ontario, Canada, K1A 0Z4, 1992.

[3] F. J. Harris, "On the use of windows for harmonic analysis with the discrete Fourier transform," *Proceedings of the IEEE*, vol. 66, pp. 51–83, January 1978.

[4] L. Li and L. B. Milstein, "Rejection of narrowband interference in PN spread-spectrum systems using transversal filters," *IEEE Transactions on Communications*, vol. 30, pp. 925–928, May 1982.

DOCUMENT CONTROL DATA

(Security classification of title, body of abstract and indexing annotation must be entered when the overall document is classified)

1. ORIGINATOR (the name and address of the organization preparing the document. Organizations for whom the document was prepared, e.g. Establishment sponsoring a contractor's report, or tasking agency, are entered in section 8.)

DEFENCE RESEARCH ESTABLISHMENT OTTAWA
NATIONAL DEFENCE
SHIRLEY BAY, OTTAWA, ONTARIO K1A 0K2 CANADA

2. SECURITY CLASSIFICATION (overall security classification of the document including special warning terms if applicable)

UNCLASSIFIED

3. TITLE (the complete document title as indicated on the title page. Its classification should be indicated by the appropriate abbreviation (S,C or U) in parentheses after the title.)

A FAST FOURIER TRANSFORM APPROACH TO INTERFERENCE SUPPRESSION IN DIRECT SEQUENCE SPREAD SPECTRUM SIGNALS (U)

4. AUTHORS (Last name, first name, middle initial)

KOZMINCHUK, BRIAN W.

5. DATE OF PUBLICATION (month and year of publication of document)

DECEMBER 1992

6a. NO. OF PAGES (total containing information. Include Annexes, Appendices, etc.)

50

6b. NO. OF REFS (total cited in document)

4

7. DESCRIPTIVE NOTES (the category of the document, e.g. technical report, technical note or memorandum. If appropriate, enter the type of report, e.g. interim, progress, summary, annual or final. Give the inclusive dates when a specific reporting period is covered.)

DREO TECHNICAL NOTE

8. SPONSORING ACTIVITY (the name of the department project office or laboratory sponsoring the research and development. Include the address.)

DEFENCE RESEARCH ESTABLISHMENT OTTAWA
NATIONAL DEFENCE
SHIRLEY BAY, OTTAWA, ONTARIO K1A 0K2 CANADA

9a. PROJECT OR GRANT NO. (if appropriate, the applicable research and development project or grant number under which the document was written. Please specify whether project or grant)

041LK11

9b. CONTRACT NO. (if appropriate, the applicable number under which the document was written)

10a. ORIGINATOR'S DOCUMENT NUMBER (the official document number by which the document is identified by the originating activity. This number must be unique to this document.)

DREO TECHNICAL NOTE 93-2

10b. OTHER DOCUMENT NOS. (Any other numbers which may be assigned this document either by the originator or by the sponsor)

11. DOCUMENT AVAILABILITY (any limitations on further dissemination of the document, other than those imposed by security classification)

(XX) Unlimited distribution
( ) Distribution limited to defence departments and defence contractors; further distribution only as approved
( ) Distribution limited to defence departments and Canadian defence contractors; further distribution only as approved
( ) Distribution limited to government departments and agencies; further distribution only as approved
( ) Distribution limited to defence departments; further distribution only as approved
( ) Other (please specify):

12. DOCUMENT ANNOUNCEMENT (any limitation to the bibliographic announcement of this document. This will normally correspond to the Document Availabilty (11). However, where further distribution (beyond the audience specified in 11) is possible, a wider announcement audience may be selected.)

UNCLASSIFIED

SECURITY CLASSIFICATION OF FORM

13. ABSTRACT (a brief and factual summary of the document. It may also appear elsewhere in the body of the document itself. It is highly desirable that the abstract of classified documents be unclassified. Each paragraph of the abstract shall begin with an indication of the security classification of the information in the paragraph (unless the document itself is unclassified) represented as (S), (C), or (U). It is not necessary to include here abstracts in both offical languages unless the text is bilingual).

(U) An FFT algorithm is examined with respect to its utility as an interference suppressor in direct sequence spread spectrum communications signals. An FFT approach is especially attractive because of its computational economy. It is this approach which has been implemented on the TMS320C30 hardware forming part of the Advanced Communications Electronic Support Measures System (ACES) and will be implemented on other high-speed hardware forming part of that system. The basic problem to be solved is described, followed by a description of the algorithm. The algorithm consists of power spectrum estimation using an FFT-based routine, interpolation of the power spectrum at equally-spaced points different from those calculated by the FFT, and design of an FIR linear phase filter which filters the data, i.e., suppresses the interference. This technique is feasible so long as the bandwidth of the interference during the observation time over which the FFT is calculated is much less than the bandwidth of the spread spectrum signal. An important result from this brief study is that the interpolation algorithm used can have an effect on the performance and reliability of the suppression filter ultimately designed and that for small order filters, the discrete Fourier transform approach may be better.

14. KEYWORDS, DESCRIPTORS or IDENTIFIERS (technically meaningful terms or short phrases that characterize a document and could be helpful in cataloguing the document. They should be selected so that no security classification is required. Identifiers, such as equipment model designation, trade name, military project code name, geographic location may also be included. If possible keywords should be selected from a published thesaurus. e.g. Thesaurus of Engineering and Scientific Terms (TEST) and that thesaurus-identified. If it is not possible to select indexing terms which are Unclassified, the classification of each should be indicated as with the title.)

Fast Fourier Transform
Direct Sequence Spread Spectrum
Spread Spectrum
Excision
Interference Suppression
Fourier Transform
Linear Phase
Finite Impulse Response
Adaptive Filter

UNCLASSIFIED

SECURITY CLASSIFICATION OF FORM